

Effect of the ionospheric irregularities occurring before earthquakes on the signal parameters of GNSS

S.A. Pulinets^{1,2}, D.V. Davidenko^{1,3}

¹Space Research Institute, Russian Academy of Sciences, Moscow

²JSC “Russian Space Systems”, Moscow

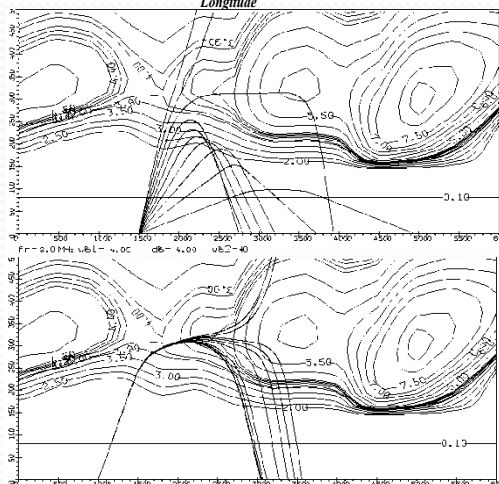
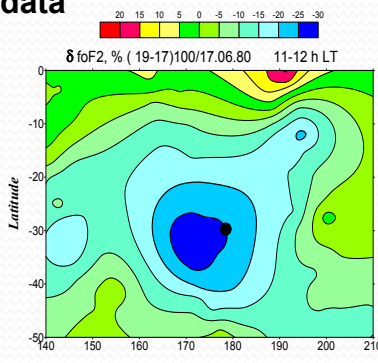
³S.P. Korolev Rocket and Space Corporation «Energia», Korolev

Outline

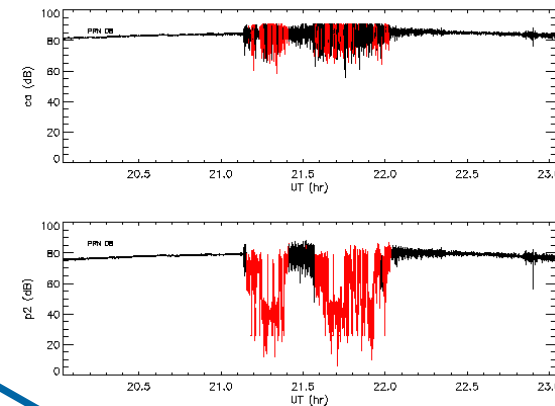
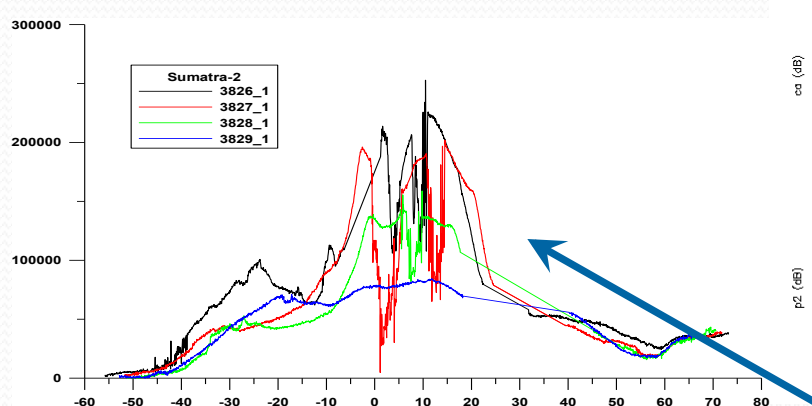
- **Introduction**
- **Seismo-ionospheric anomalies – unpredictable threats for the satellite navigation and communication**
- **The types of seismo-ionospheric anomalies**
- **Multi-parameter monitoring – the way to anticipate the seismo-ionospheric anomalies in advance**
- **Local character and self-similarity of the ionospheric precursors – the way to their automatic recognition**
- **Conclusions**

Seismo-ionospheric anomalies and radio waves propagation

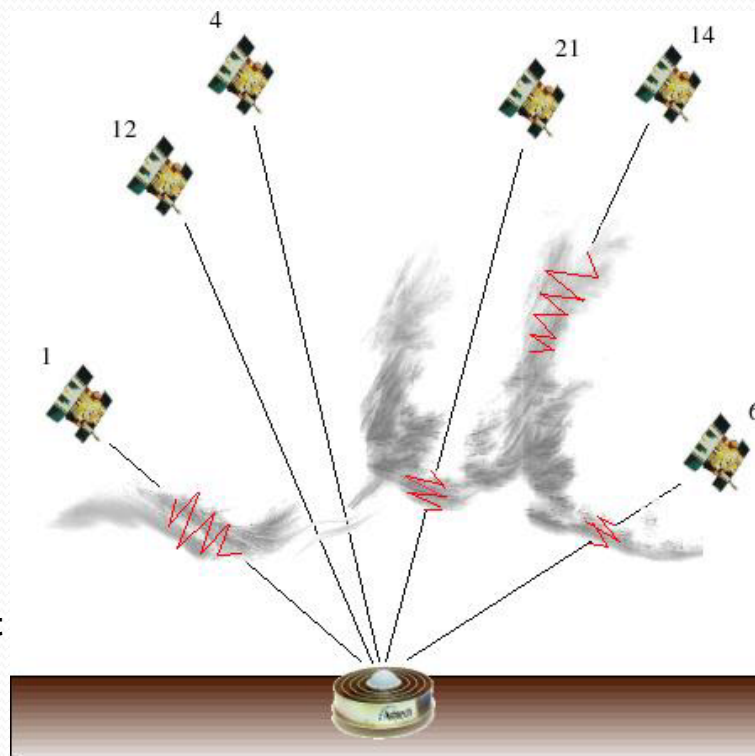
The «hole» in the ionosphere over the earthquake preparation zone in New Zealand region by Intercosmos-19 data



Anomalous trajectories of HF waves propagation under different incidence angles on the modified area

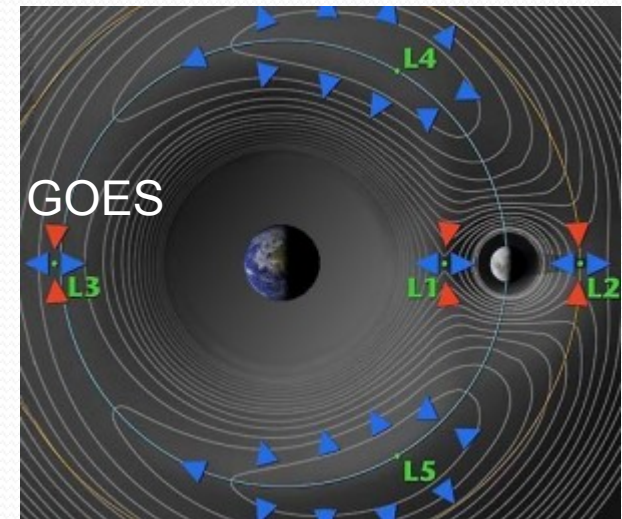


Plasma bubbles formation before the M8.6 Sumatra earthquake 27 March 2005 by the DEMETER satellite data



Plasma bubbles effect is the signal scintillation up to complete loss of tracking the GPS signal (tracking)

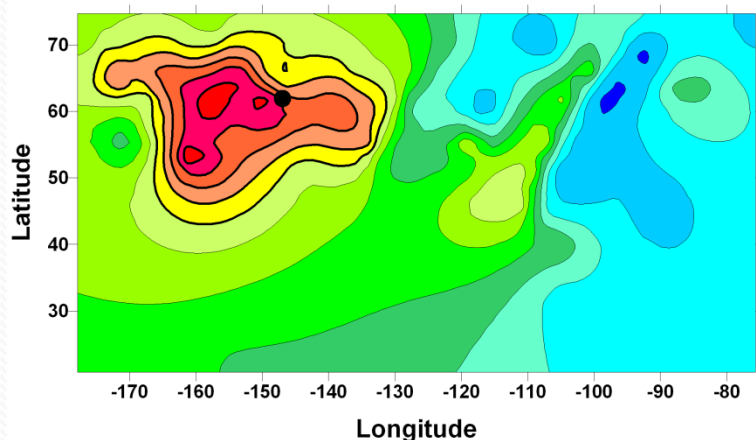
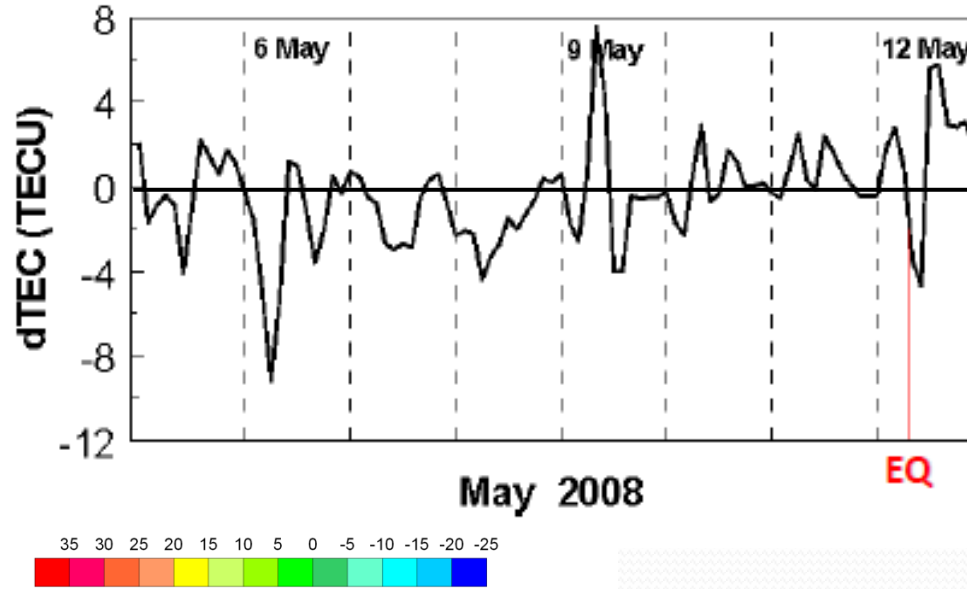
unpredictable threats for the satellite navigation and communication



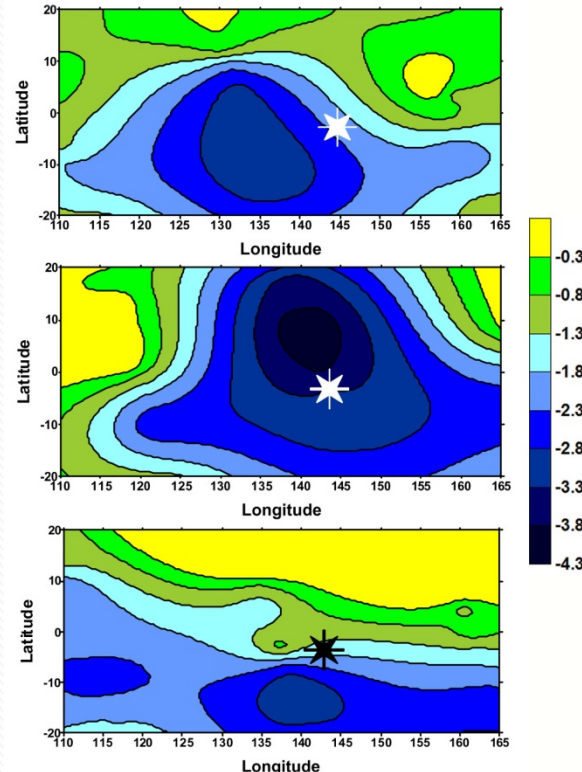
Solar flare – 8.3 min
X-rays – few hours
CMEs – 2-3 days

Nobody knows where and when the next earthquake will happen and seismo-ionospheric anomaly will form

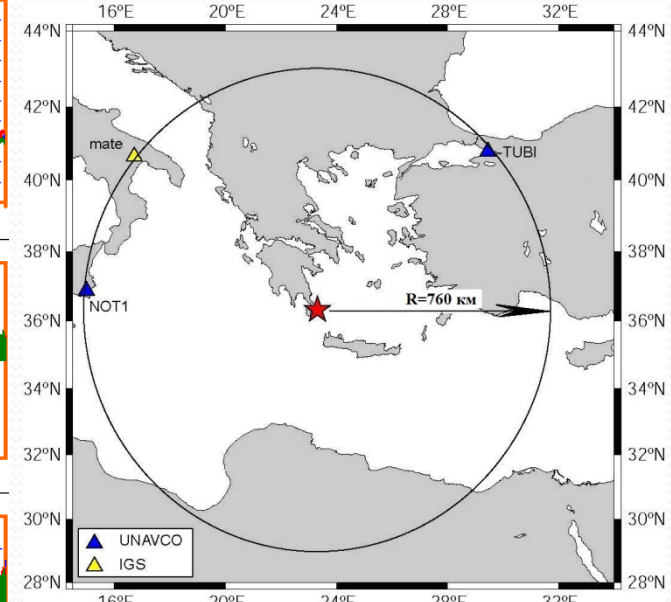
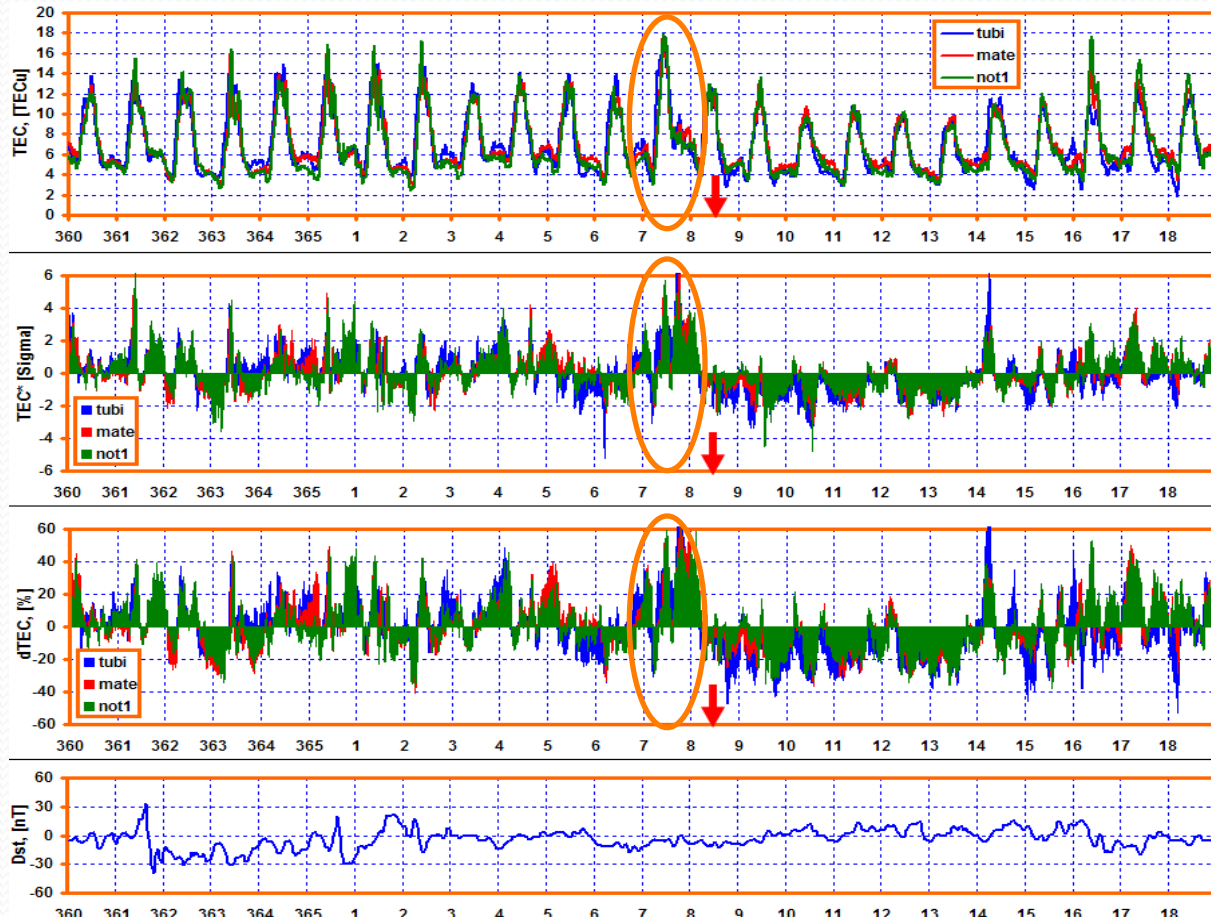
How look like the seismo-ionospheric anomalies



Positive and negative deviations are possible



In GPS TEC language for GPS receivers located inside of the earthquake preparation zone



- $dTEC = 100 \cdot (TEC - TEC_{CP}) / TEC_{CP}$

TEC, [TECu] – value of TEC for given time;

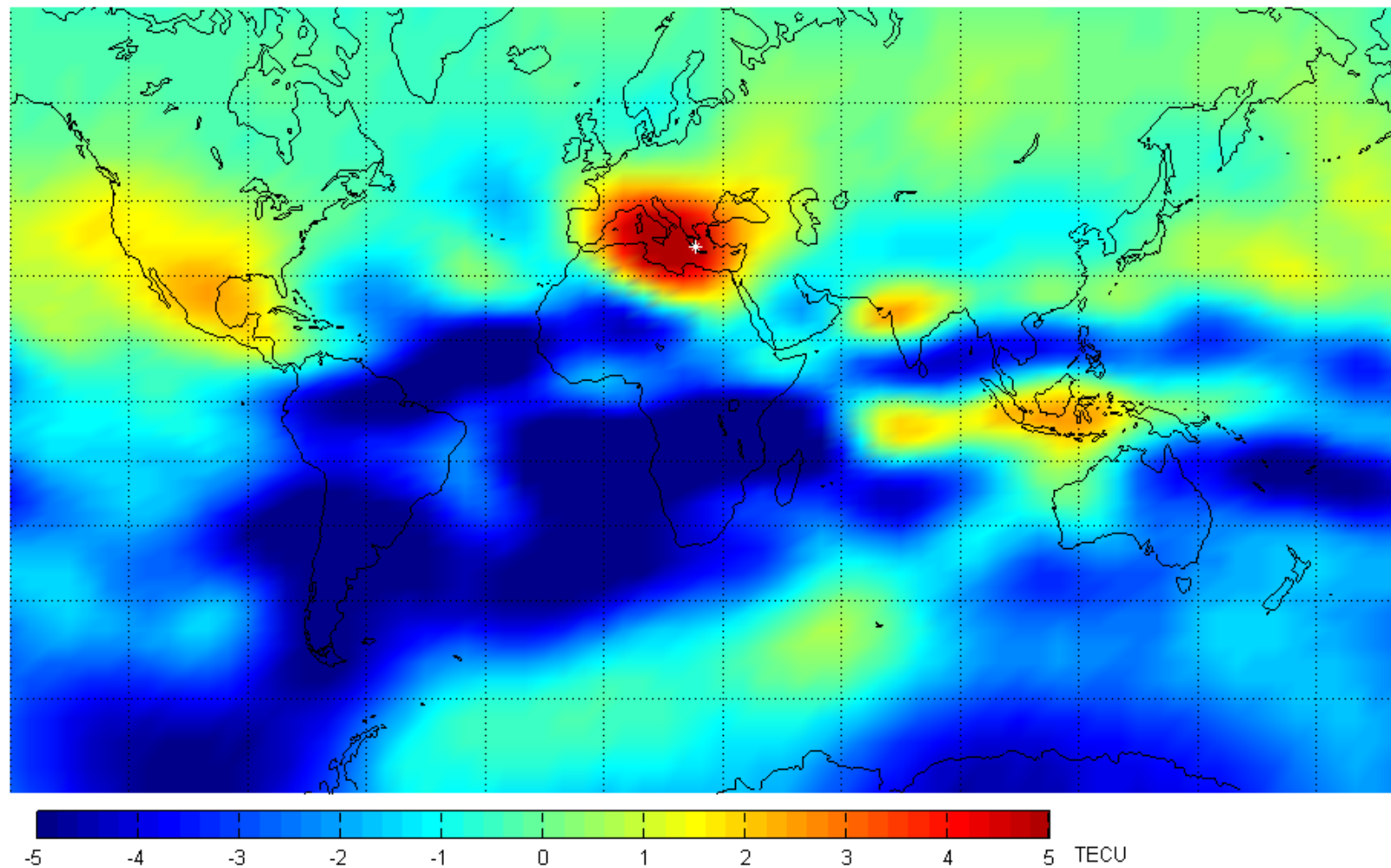
TEC_{CP} , [TECu] – running average value of TEC calculated for 15 previous values TEC for given time;

σ – standard deviation calculated for 15 previous values of TEC for given time.

How it looks at GIM map

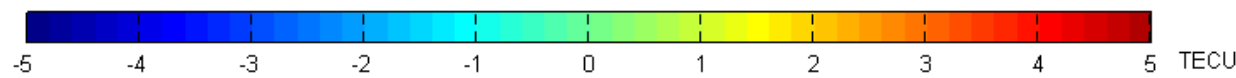
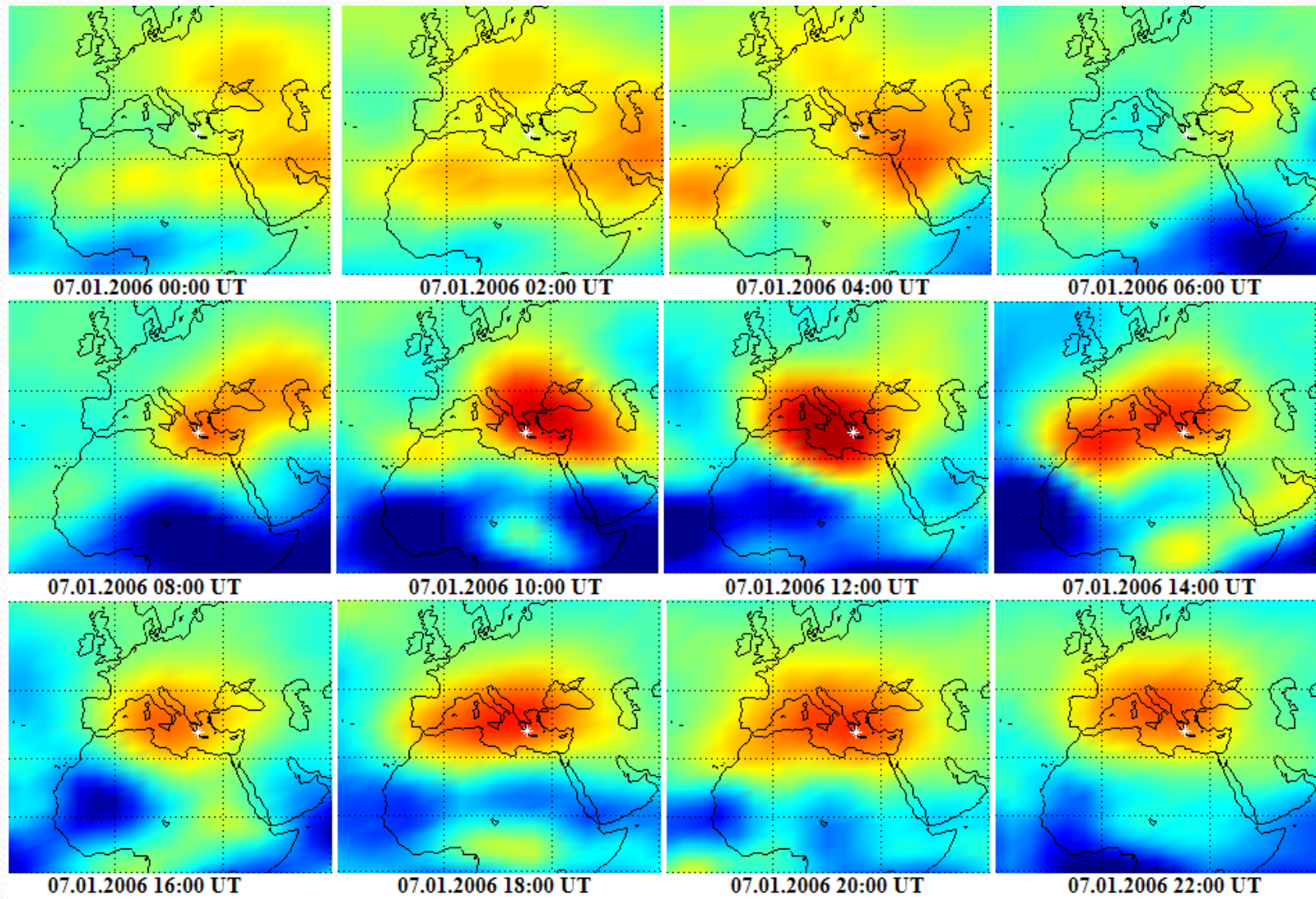
TEC difference with previous 15-days mean

Source: IGS Center: Athens 2006 Date: 2006.01.07 UT: 12:00:00 LT: 13.5



Region with considerable increase of TEC over the epicenter 24 h before the earthquake M6.7.

How long it can exist



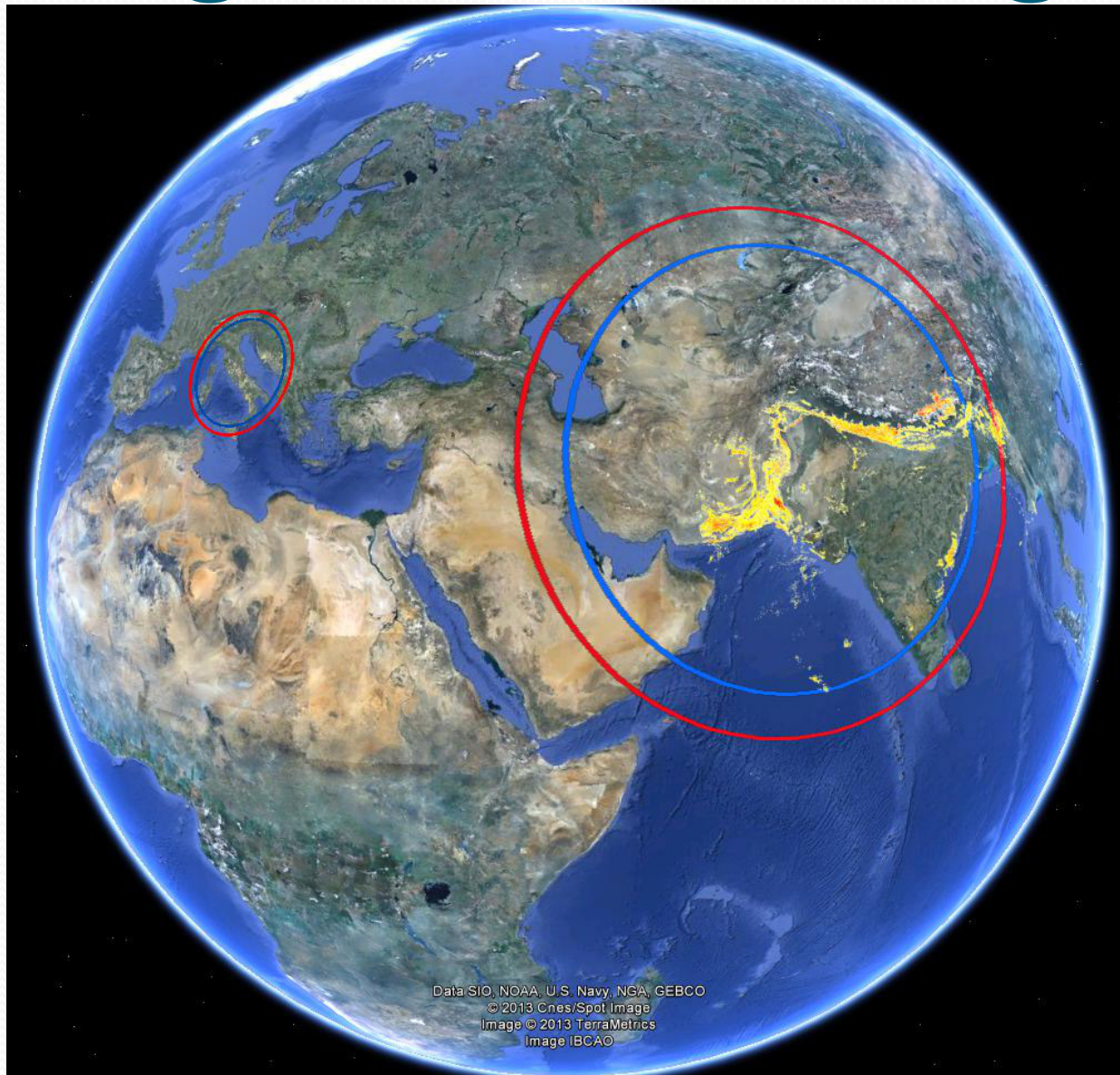
How large

$$R=10^{0.43M} \text{ km} \sim 511 \text{ km}$$



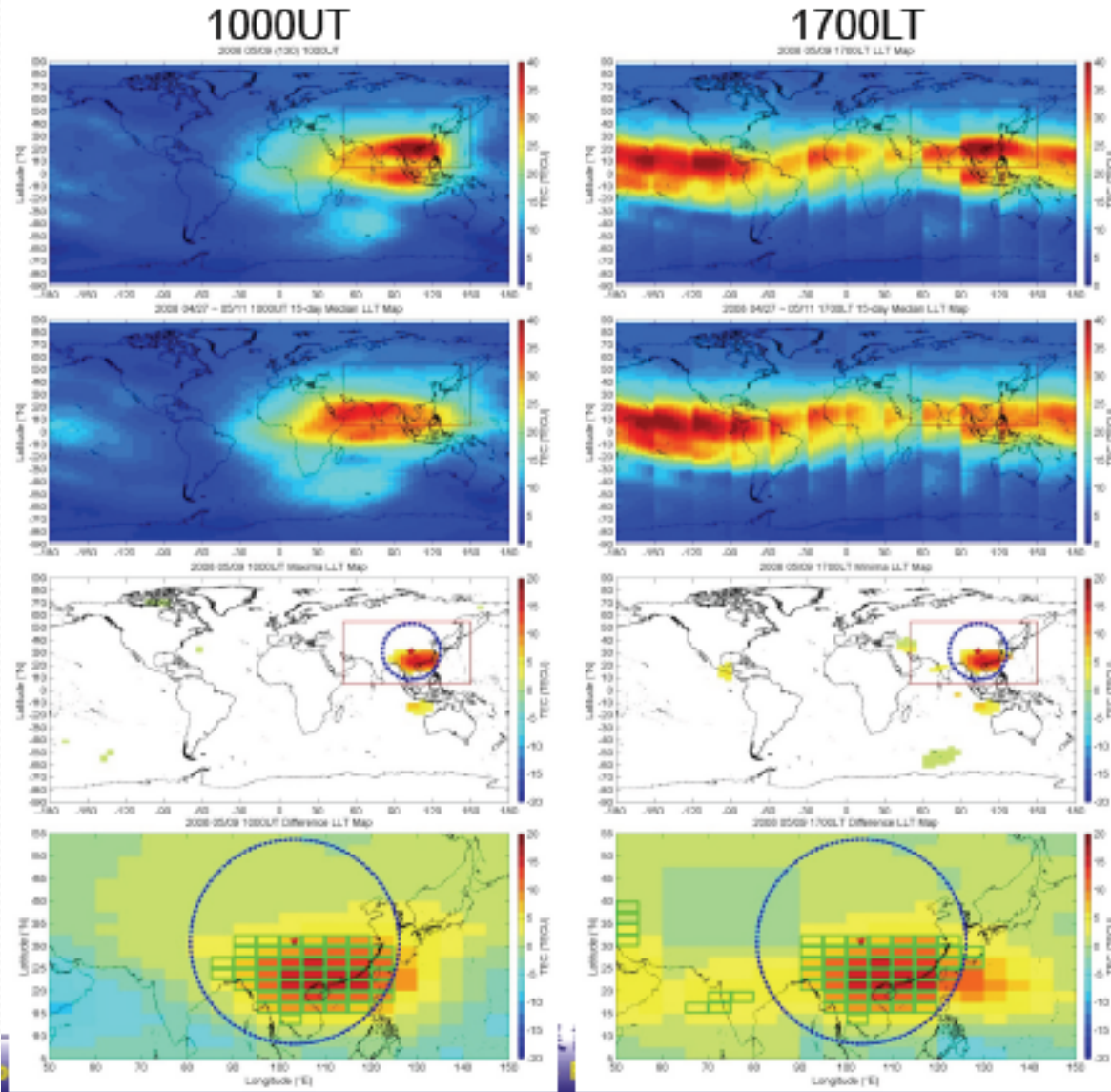
Magnitude	3	4	5	6	7	8	9
Earthquake preparation zone radius ρ (km)	19.5	52.5	141	380	1022	2754	7413

Magnitude scaling



Data SIO, NOAA, U.S. Navy, NGA, GEBCO
© 2013 Cnes/Spot Image
Image © 2013 TerraMetrics
Image IBCAO

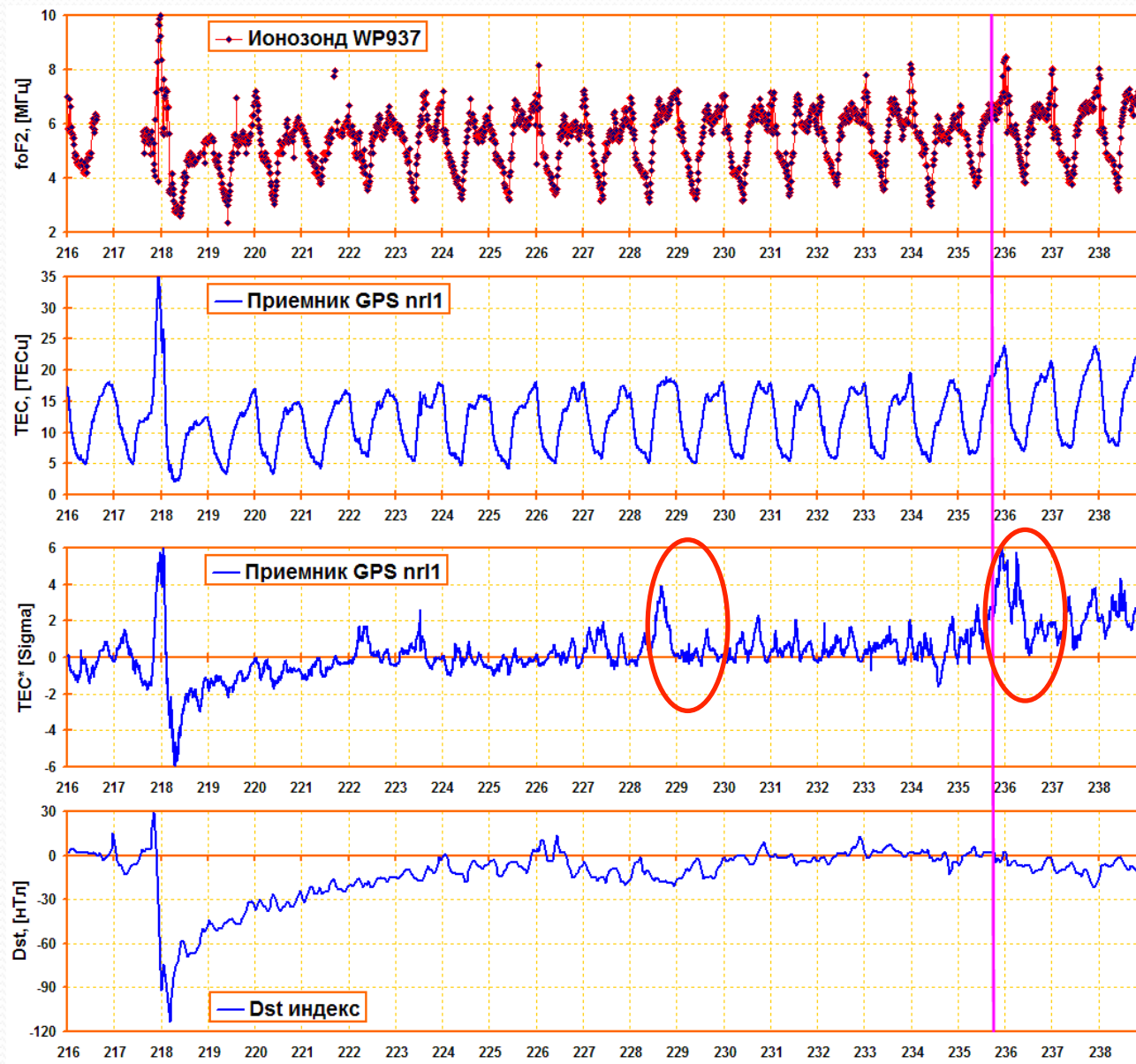
Wenchuan earthquake



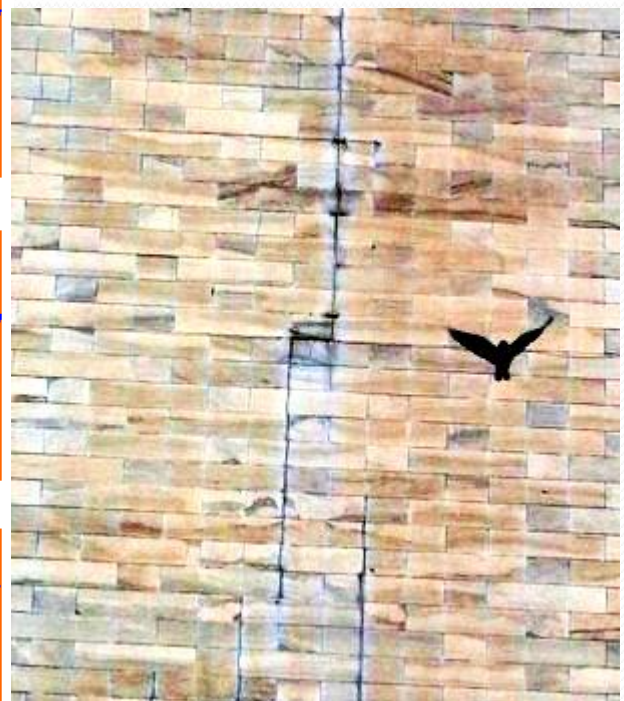
The GIMs observed at 08:00UT and global fixed 15:00 LT on day 3 before the 2008 Mw7.9 Sichuan Earthquake.

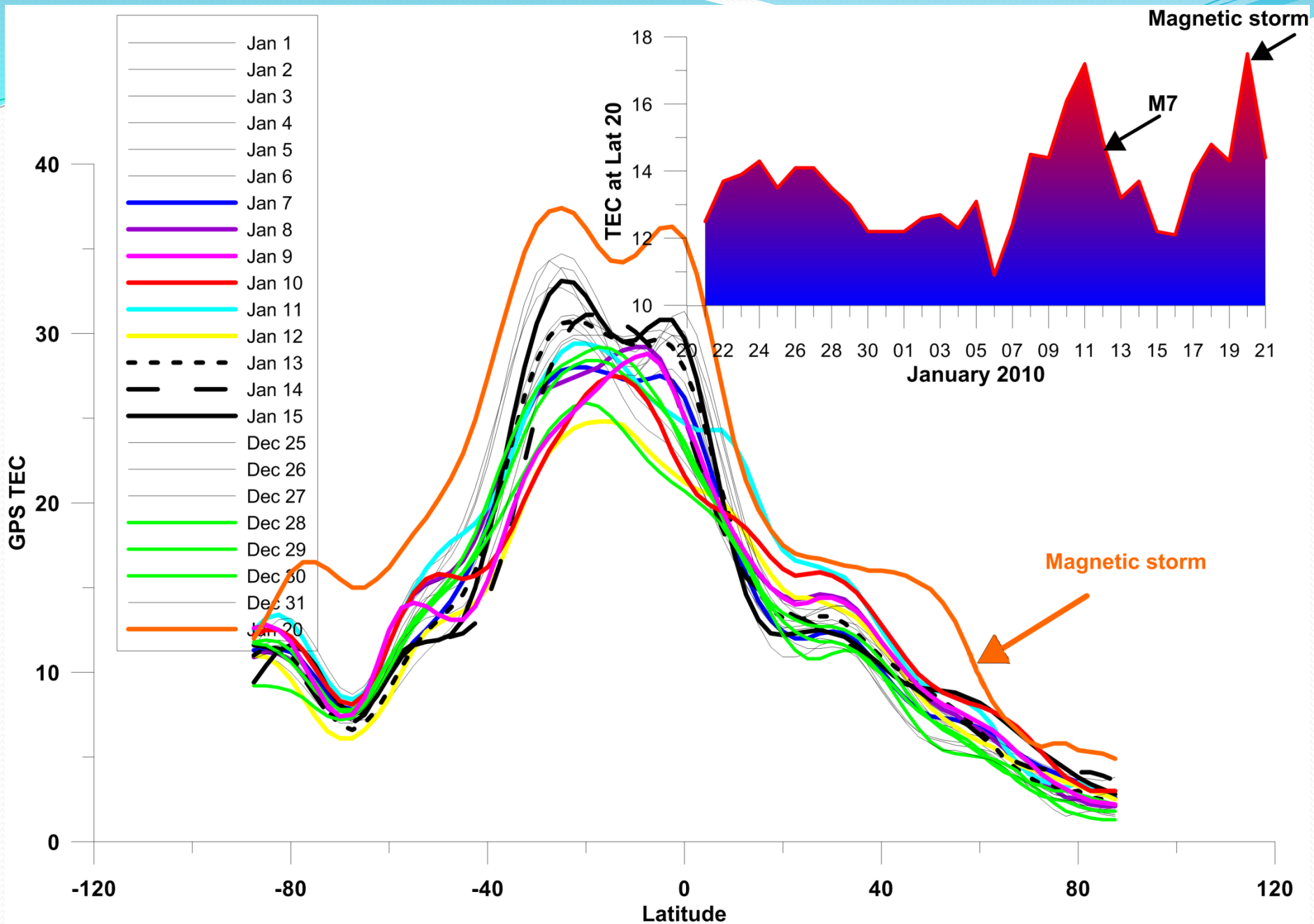
Liu et al., 2013

Magnetic storm and earthquake



Virginia M5.8 earthquake
23 August 2011

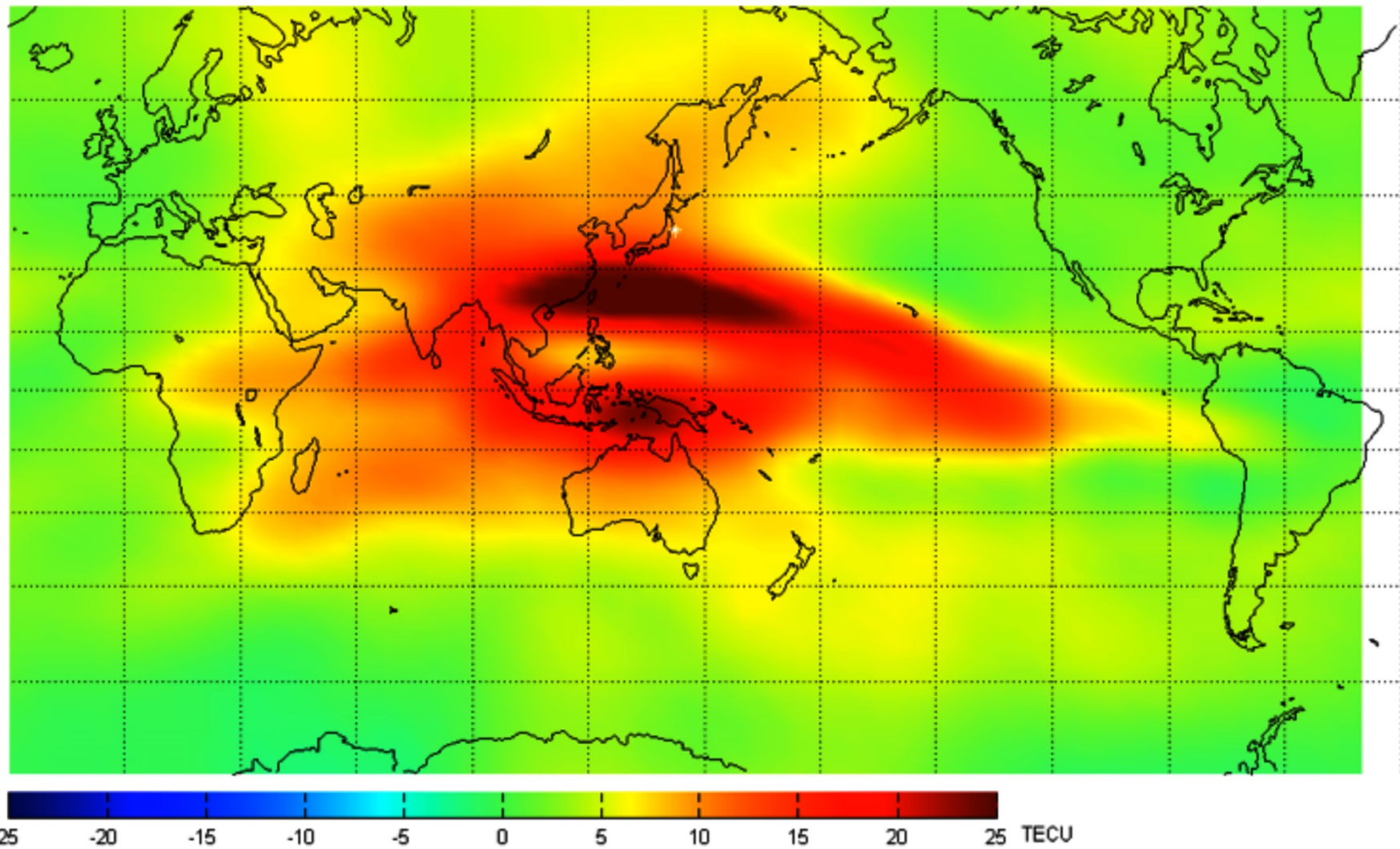




38.3 N
142.4 E

Tohoku earthquake

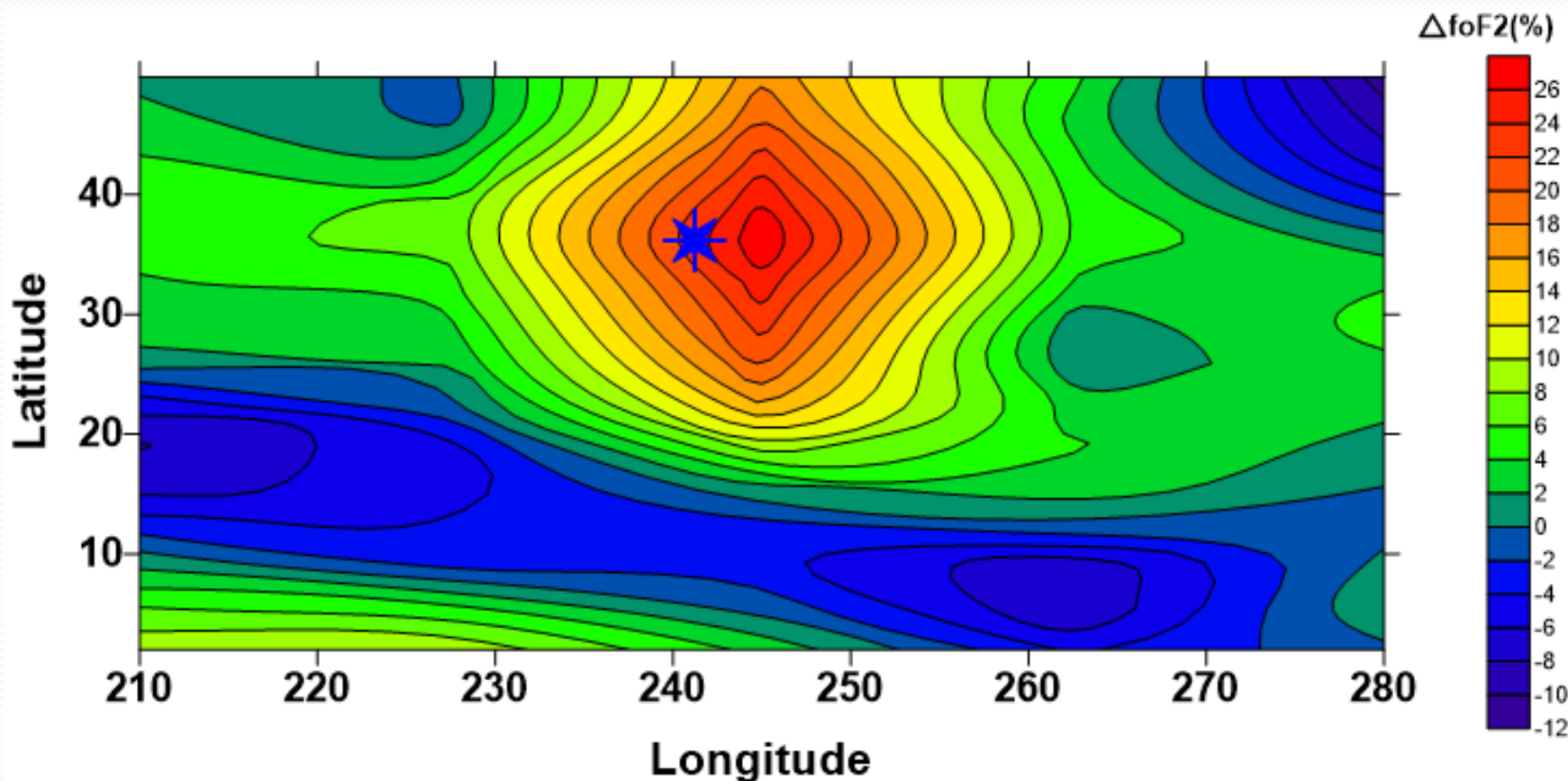
TEC difference with previous 15-days mean
Source: IGR Center: Sendai Date: 2011.03.08 UT: 06:00:00 LT: 15.5

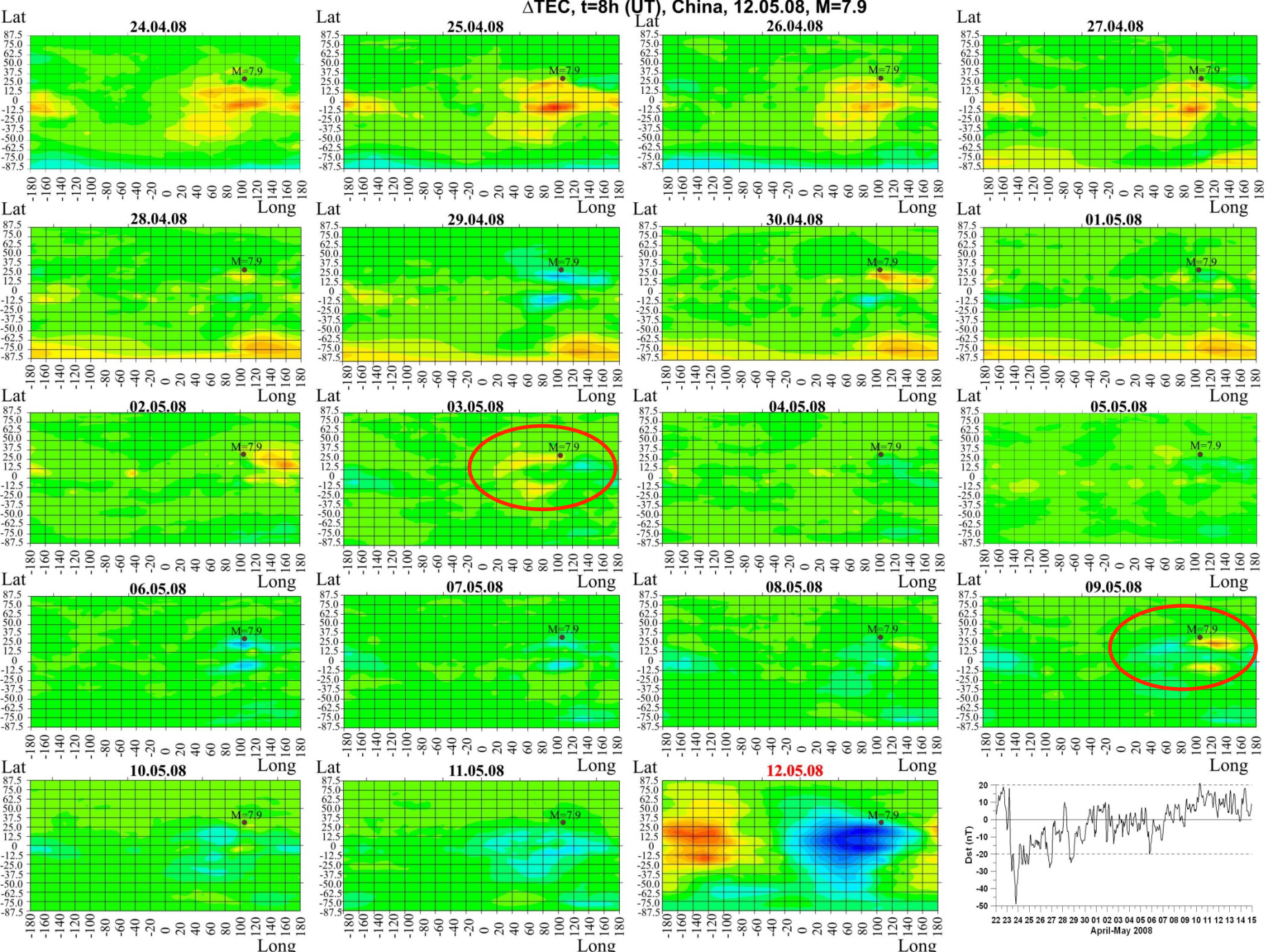


Equatorial anomaly reaction on the middle latitude earthquakes

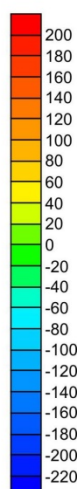
Mammoth Lake seismic swarm,
May 25-27, 1980, 4 shocks M>6

37.5 N
118.8 W



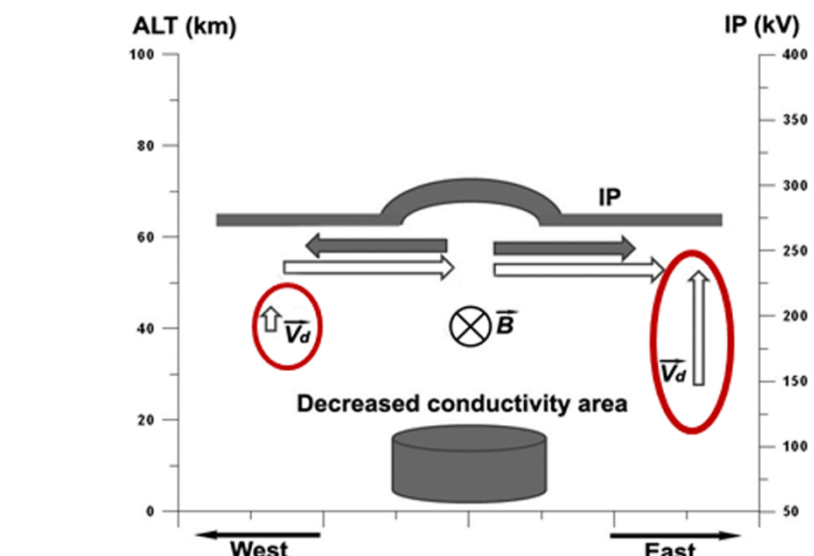
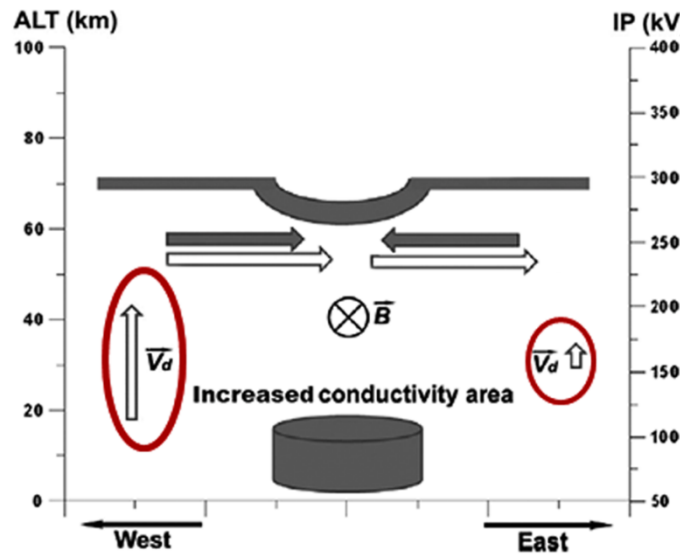
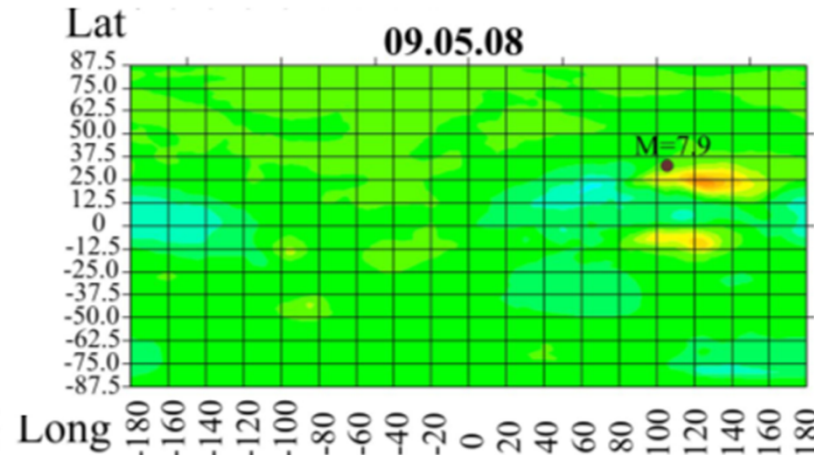
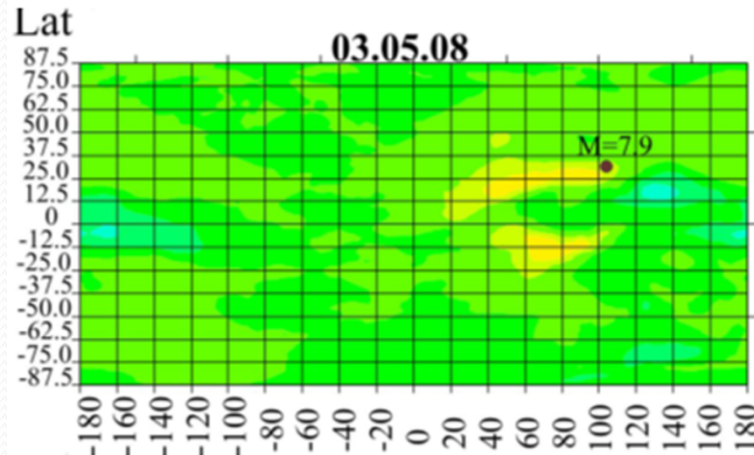


22 23 24 25 26 27 28 29 30 01 02 03 04 05 06 07 08 09 10 11 12 13 14 15
April-May 2008



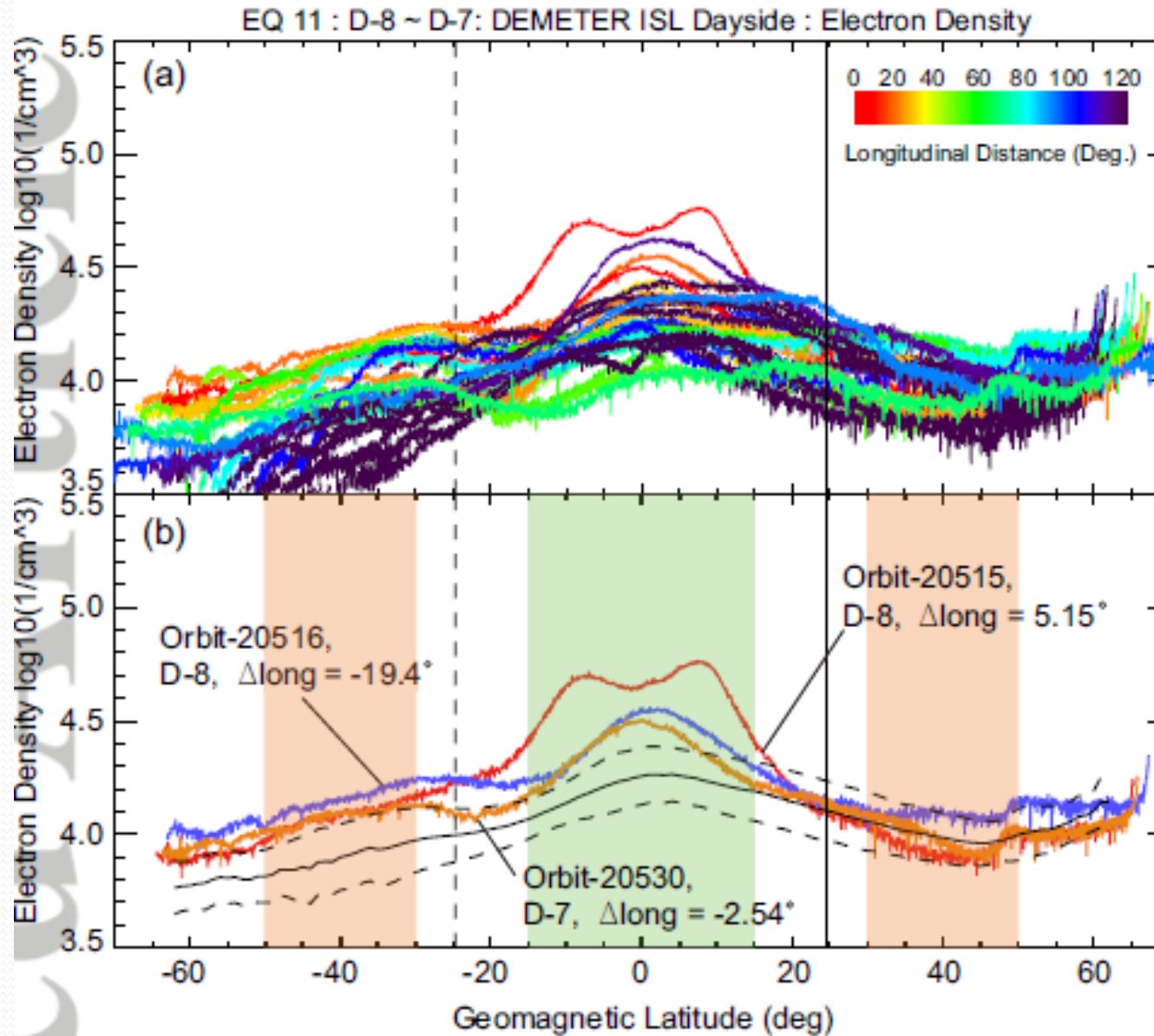
Ionospheric potential variations

Pulinets and Davidenko, 2014

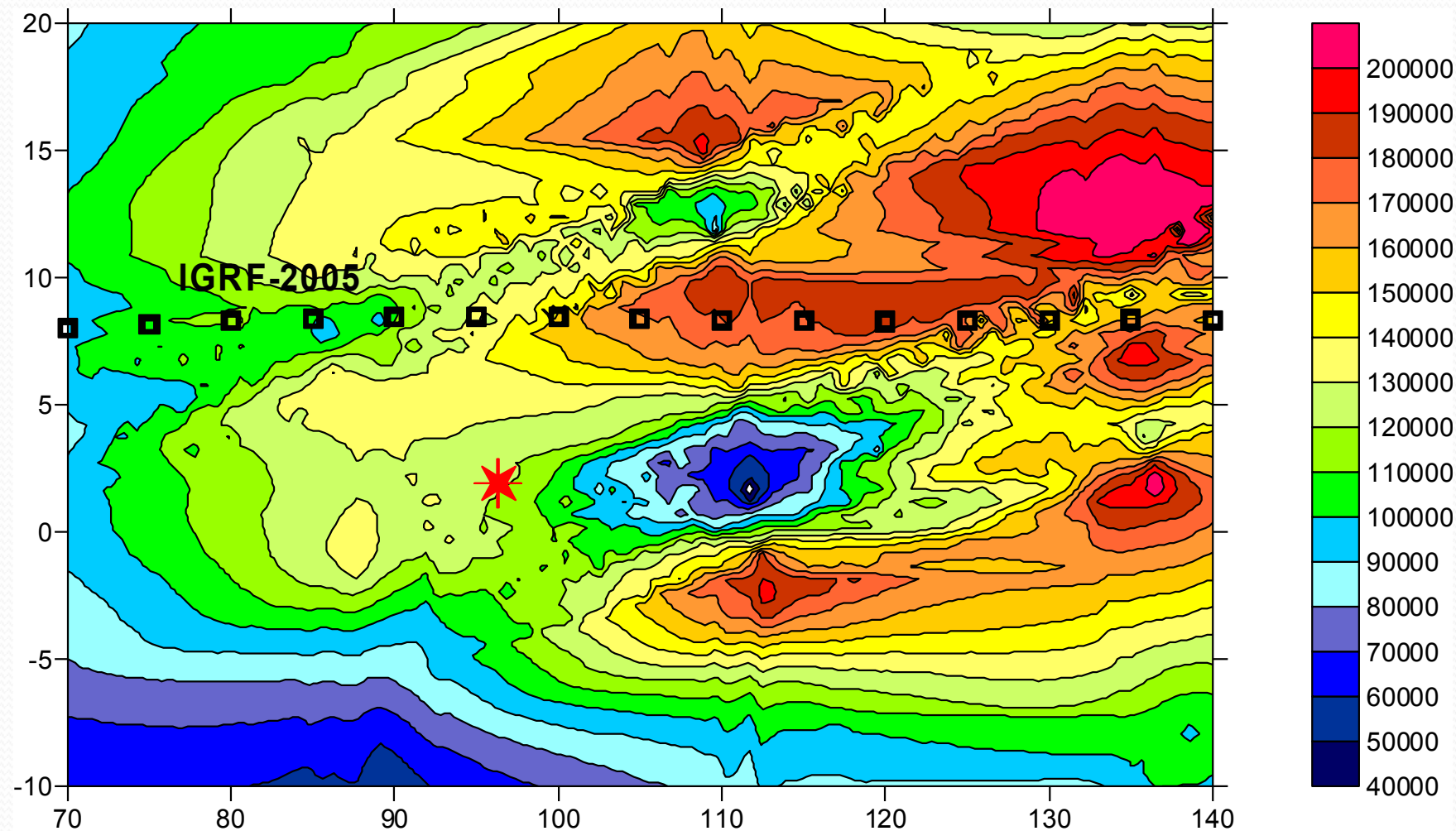


Pure anomalous electric field effect

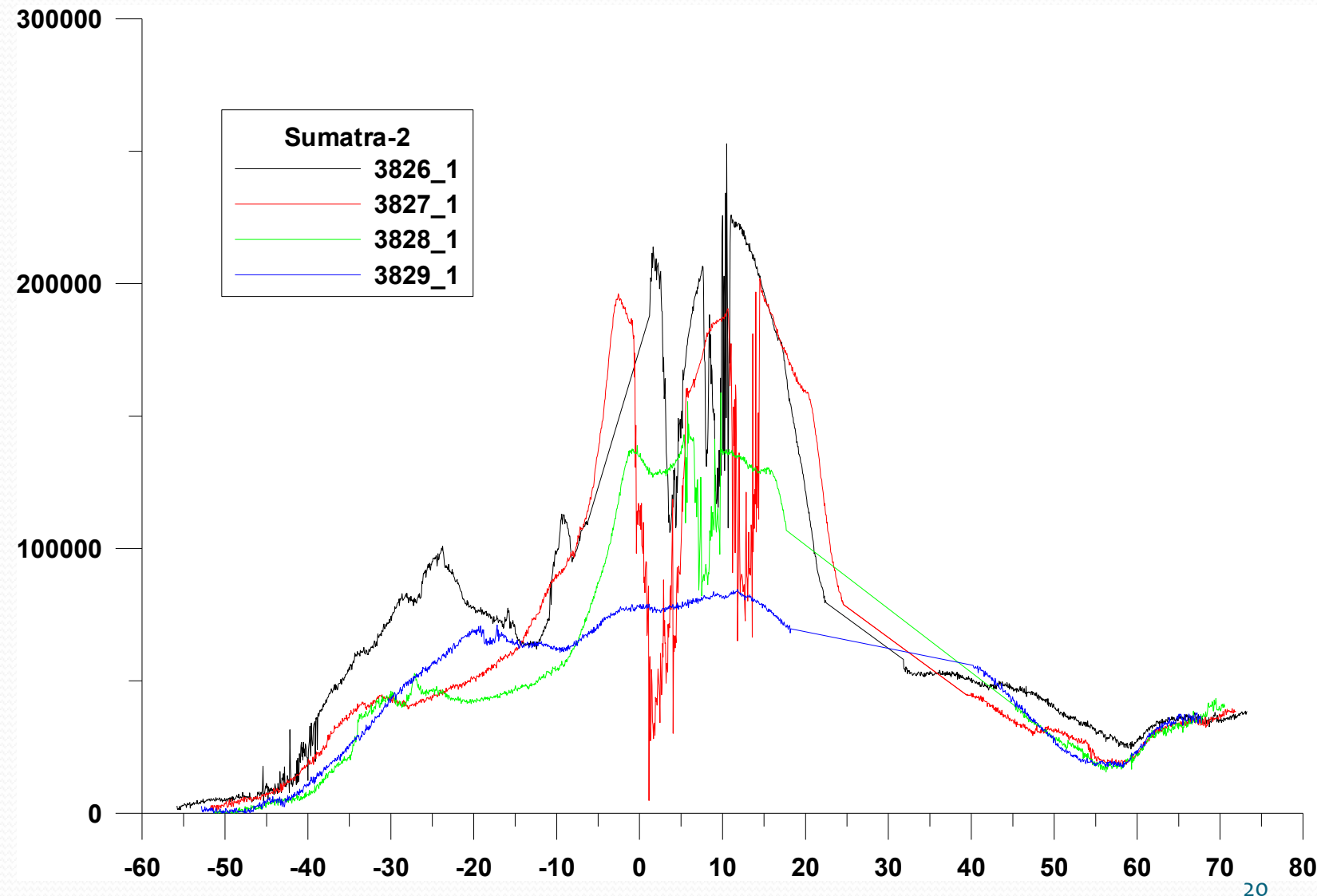
Ryu et al, JGR, 2014, accepted



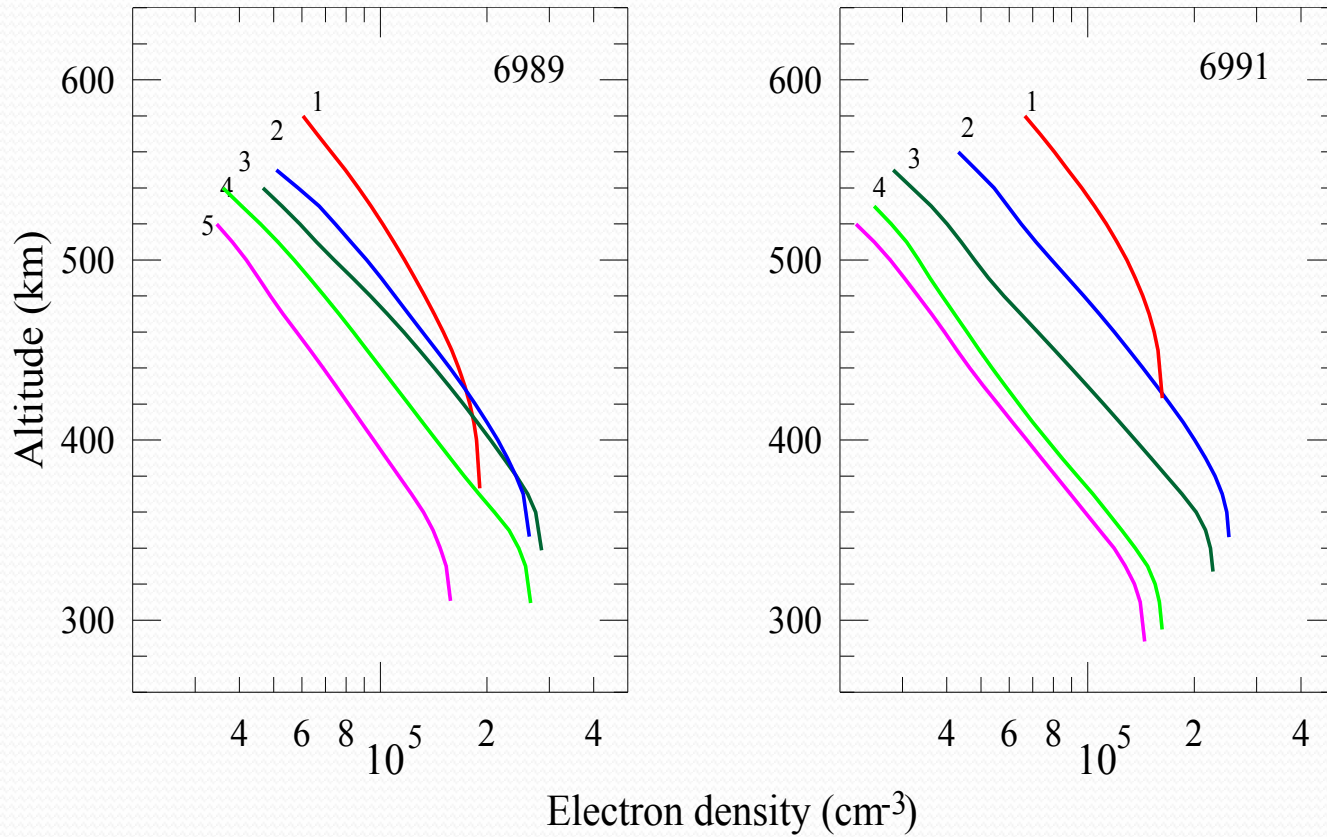
Ion concentration distribution before Sumatra M8.7 EQ of 27 March 2005



Plasma bubbles

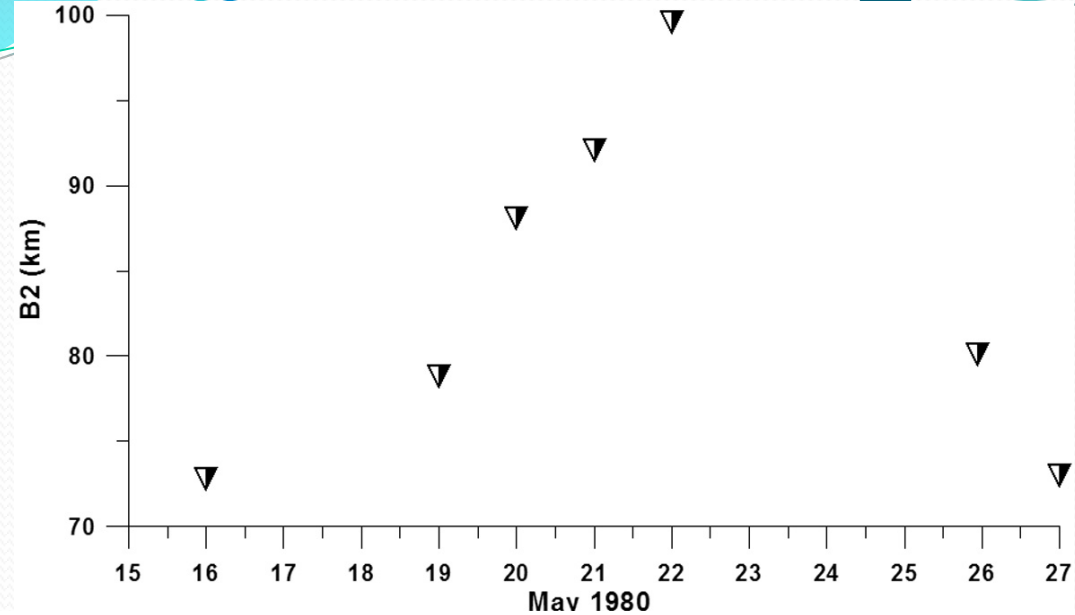


Vertical profiles modification

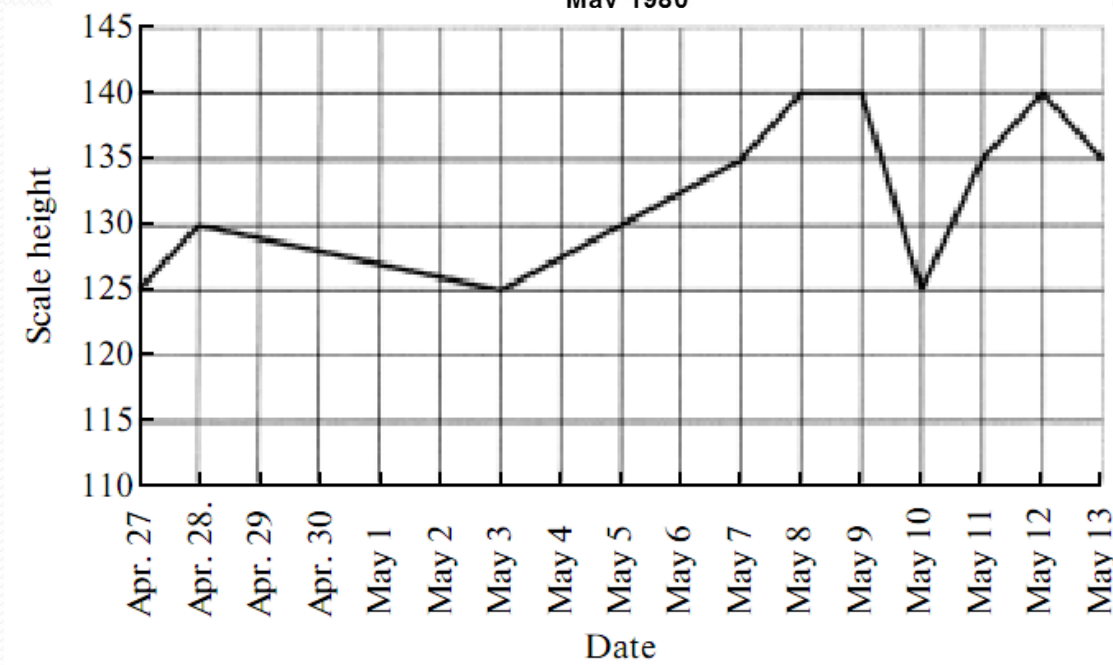


	lat	hmF2	foF2	B2u	k2u		lat	hmF2	foF2	B2u	k2u
1.	8.4	375	12.4	75.8	0.02	1.	9.6	425	11.5	61.7	0.17
2.	0.6	345	14.6	47.1	0.14	2.	1.8	345	14.2	47.5	0.12
3.	-3.3	340	15.2	43.3	0.13	3.	-2.2	325	13.5	40.6	0.12
4.	-7.2	310	14.6	44.4	0.12	4.	-10.0	295	11.4	44.6	0.13
5.	-15.1	310	11.3	46.5	0.15	5.	-14.0	290	10.8	48.4	0.11

Scale Height variations

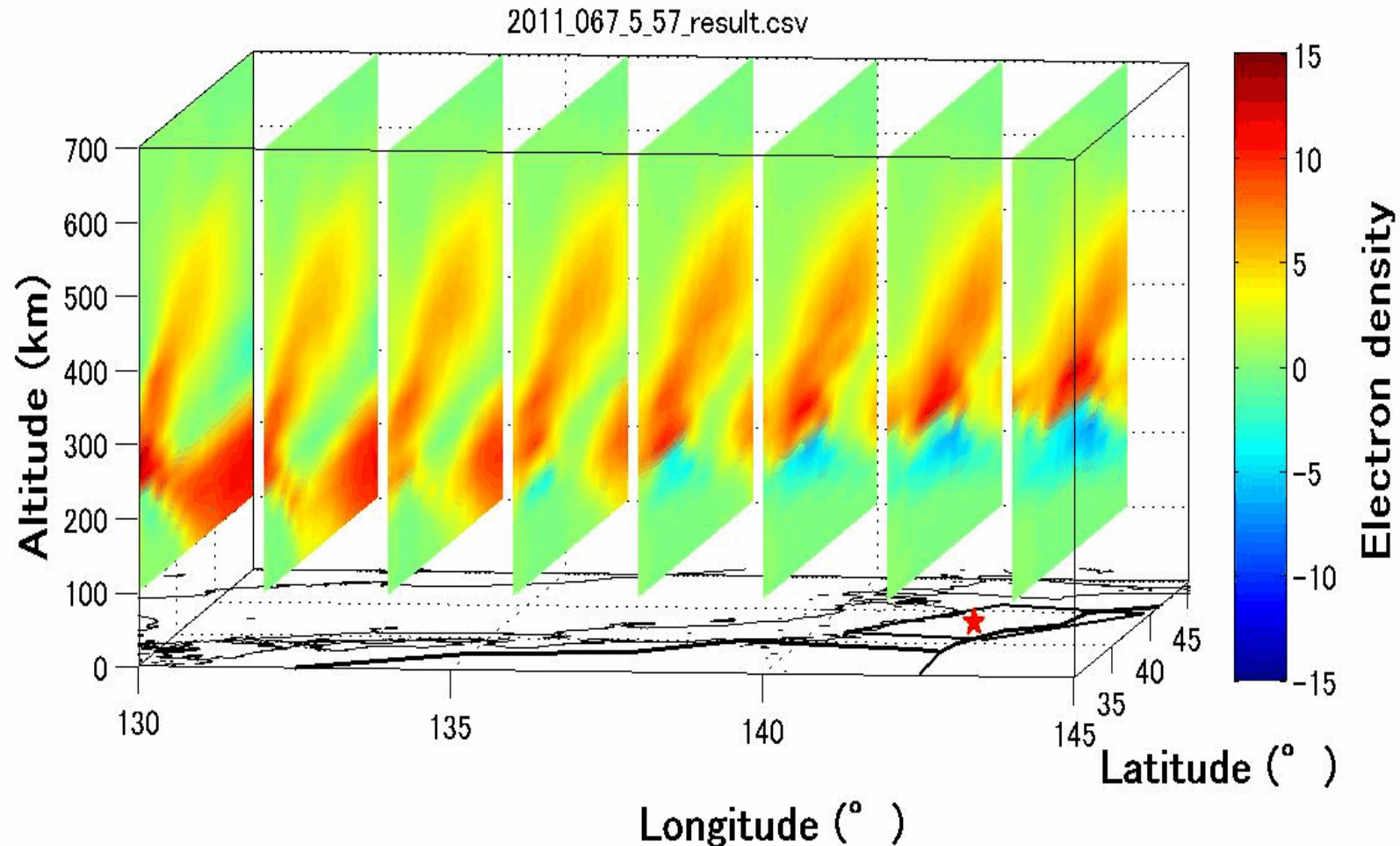


Mammoth Lake
May 1980, USA

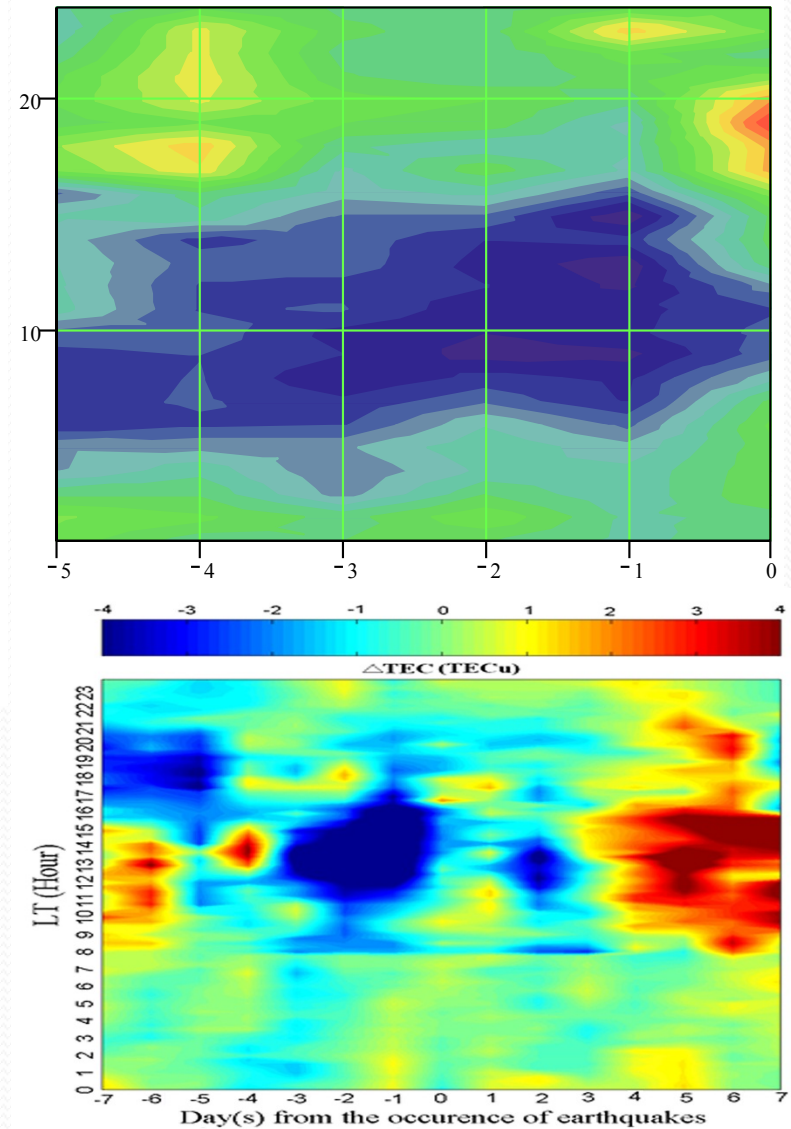
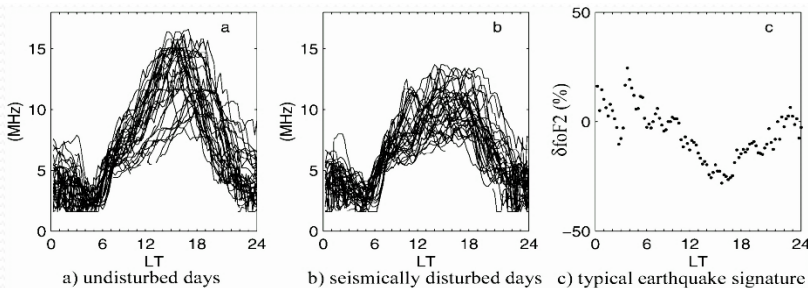
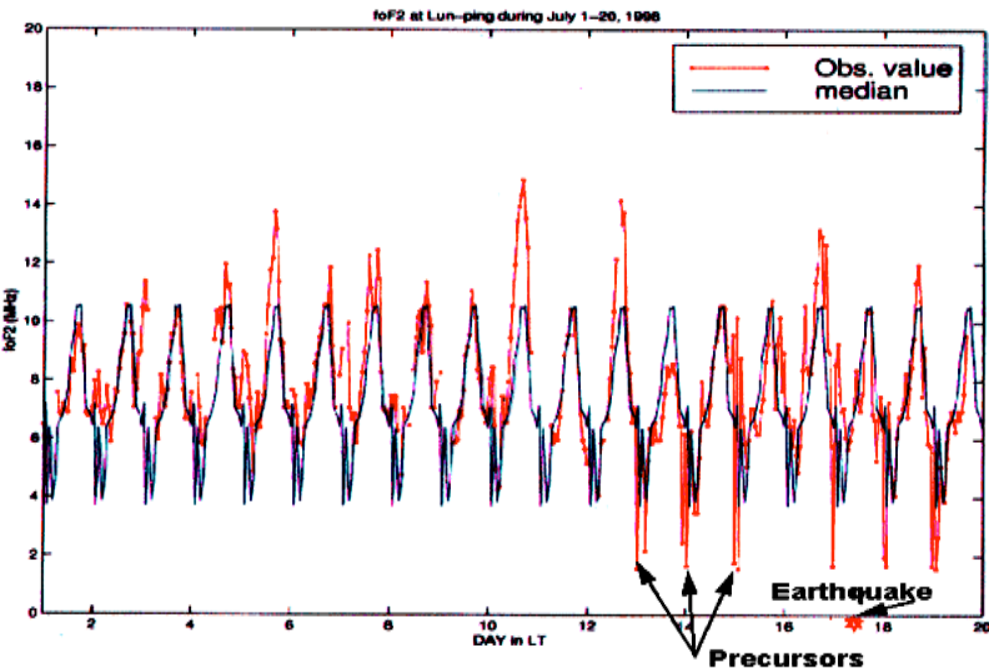


Wenchuan
May 2008, China

Tohoku, 2011, tomography



Self similarity of earthquake precursors



Formal determination of self similarity

We represent the state of the ionosphere prior to the event in the form of an A_{ij} matrix whose columns contain the hourly deviations of f_0F2 from its median value. The number of columns in the matrix is determined by an expected time interval between a precursor and an event. In this paper, we assume that this interval does not exceed six days and, respectively, the dimension of the A_{ij} matrix is 24×6 , i.e., $i = 1 \dots 24, j = 1 \dots 6$.

For all events we form matrices in the same manner and obtain an $A_{ij}^{(n)}$ series, where n is the ordinal number of an event. We now introduce the value

$$S_n = \frac{\sum_{i,j} \langle A_{ij}^{(n)} \rangle_n^2}{\langle \sum_{i,j} (A_{ij}^{(n)})^2 \rangle_n},$$

where $\langle \dots \rangle_n$ means averaging over an ensemble of n events. S_n is the dispersion normalized so that $S_1 = 1$.

With the help of S_n , it is convenient to characterize the degree of $A_{ij}^{(n)}$ similarity at various n . For example, if $A_{ij}^{(n)}$ values for various events do not correlate with one another, the S_n series tends to unity at $n \rightarrow \infty$. In the other extreme case, when the states of the ionosphere prior to all events are completely identical, S_n increases: $S_n \sim n$ at $n \rightarrow \infty$.

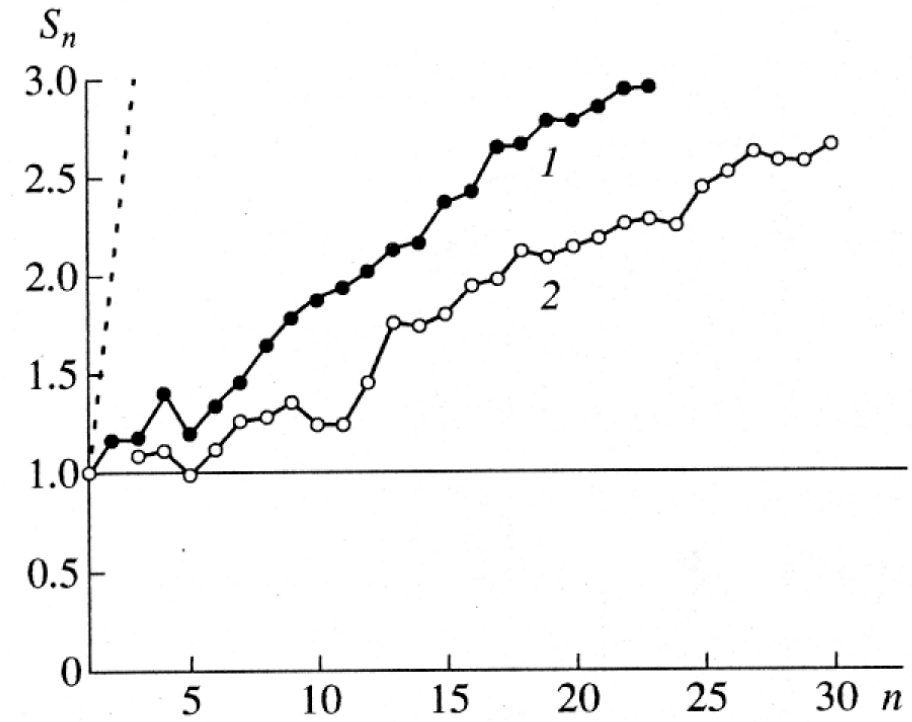
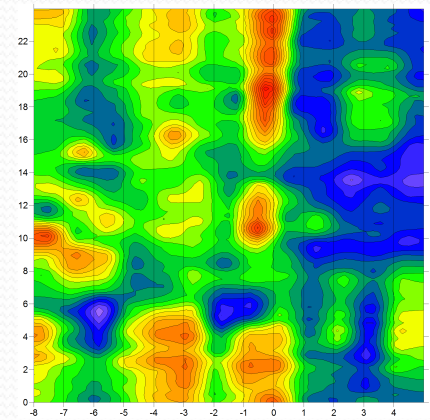
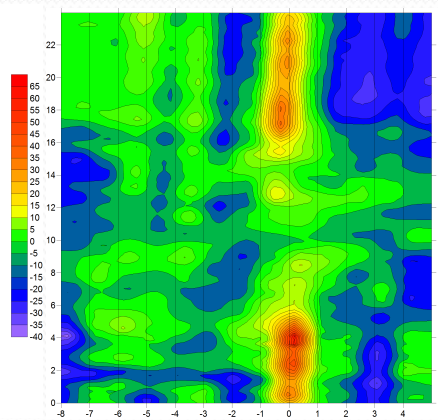


Fig. 2. Behavior of the S_n parameter for two groups of deep-focus earthquakes: a series of 23 (curve 1) and 30 (curve 2) events. Dashed and solid curves: theoretical curves for a similar state and noncorrelated states of the ionosphere prior to any earthquake in the series, respectively.

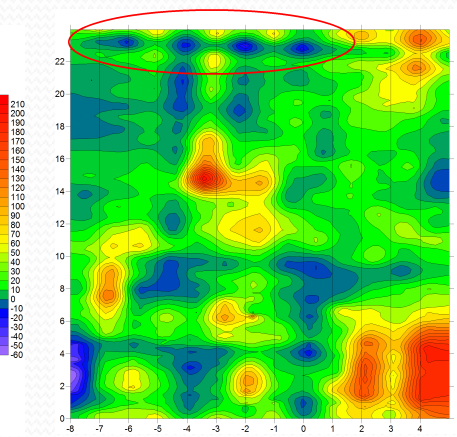
Characteristic patterns of the ionospheric precursor



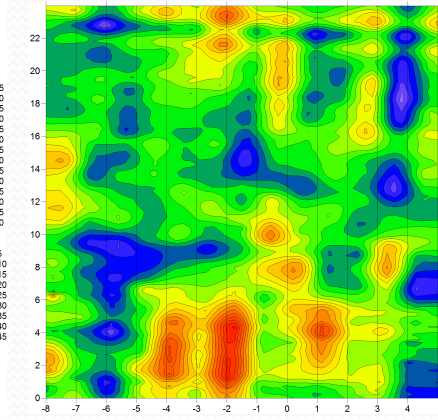
EQ G1



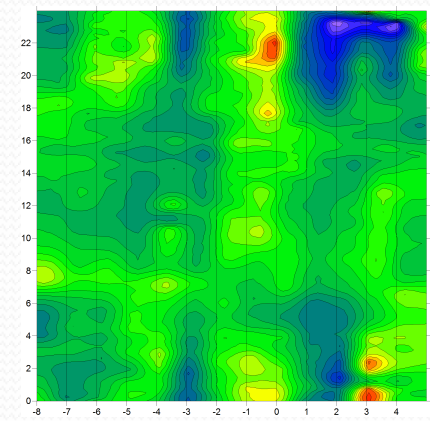
EQ G2



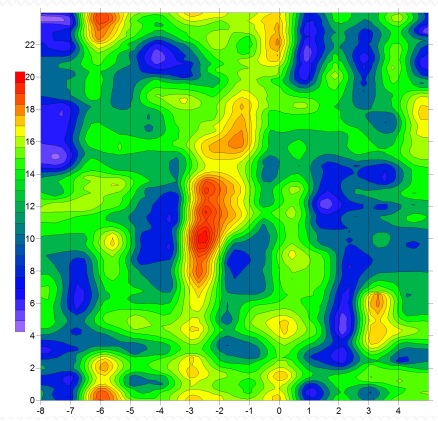
EQ G3



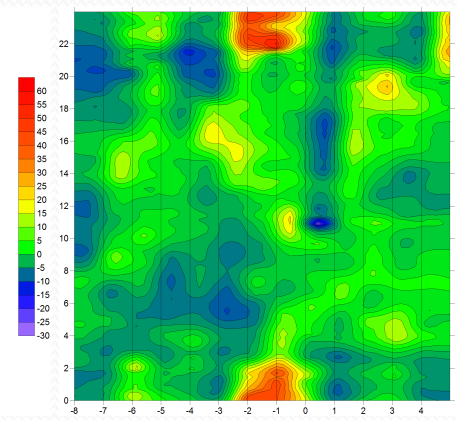
EQ G4



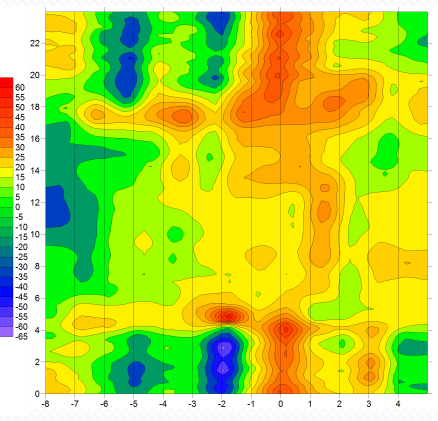
EQ G5



EQ G6

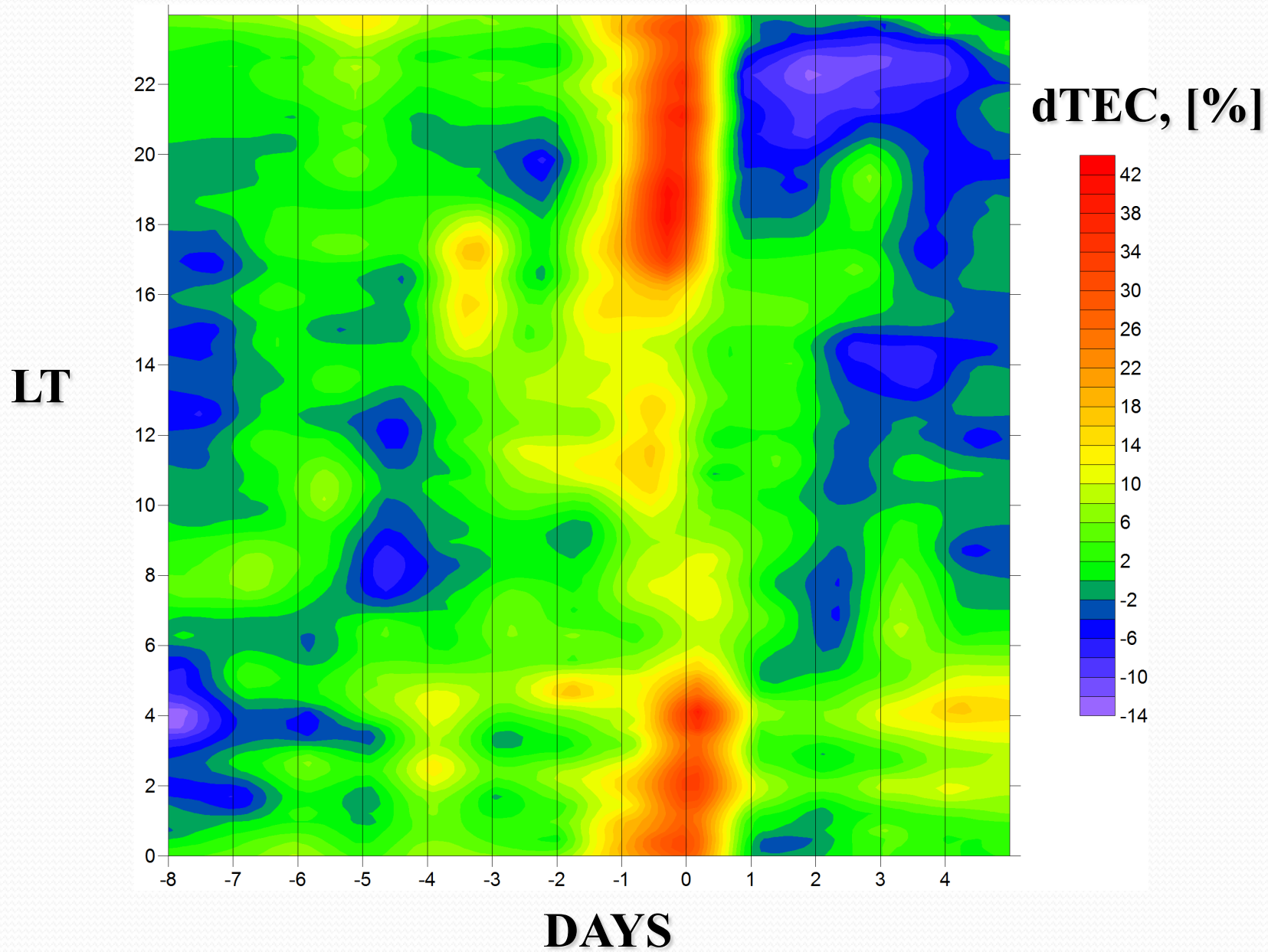


EQ G7

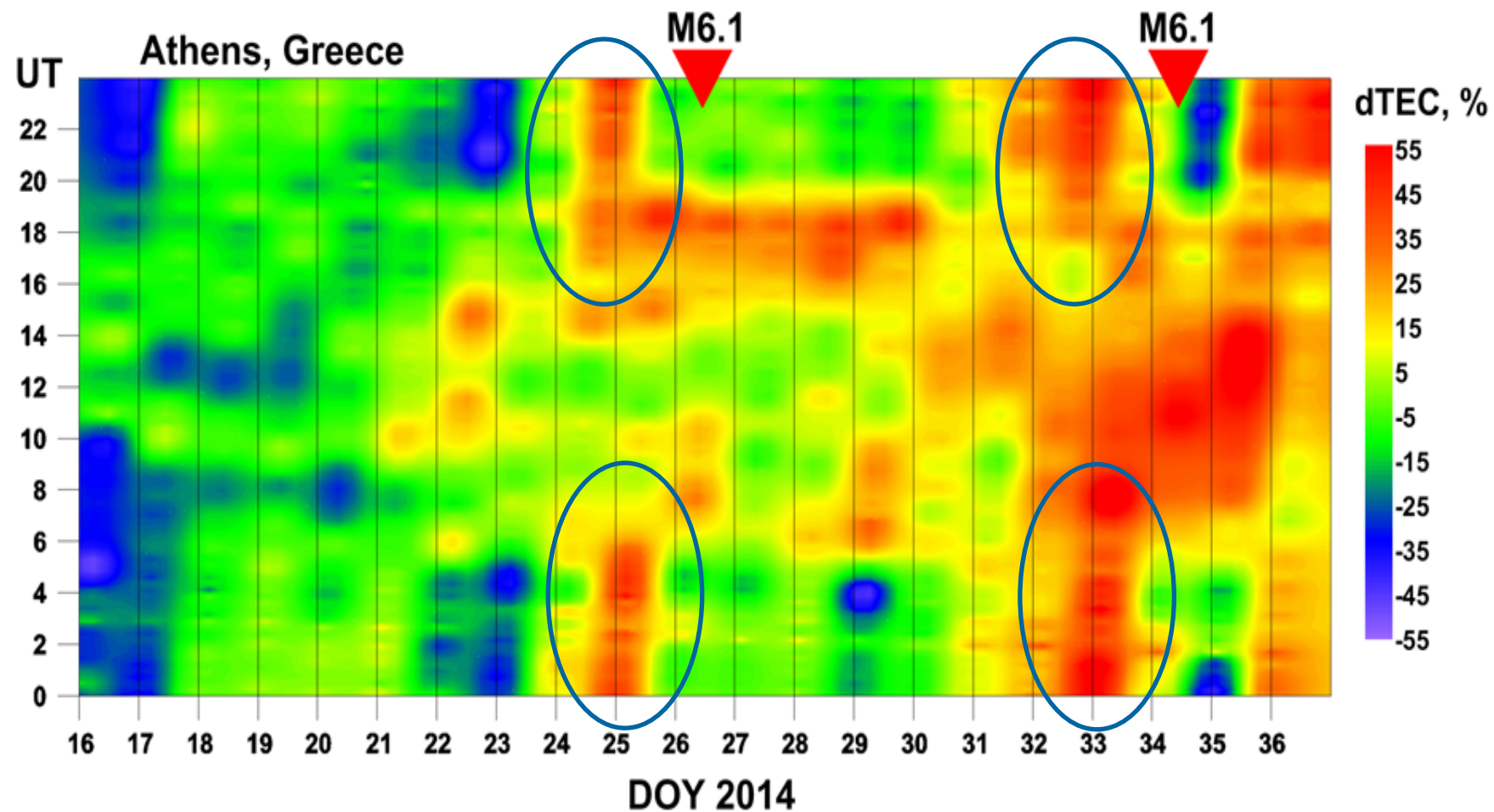


EQ G8

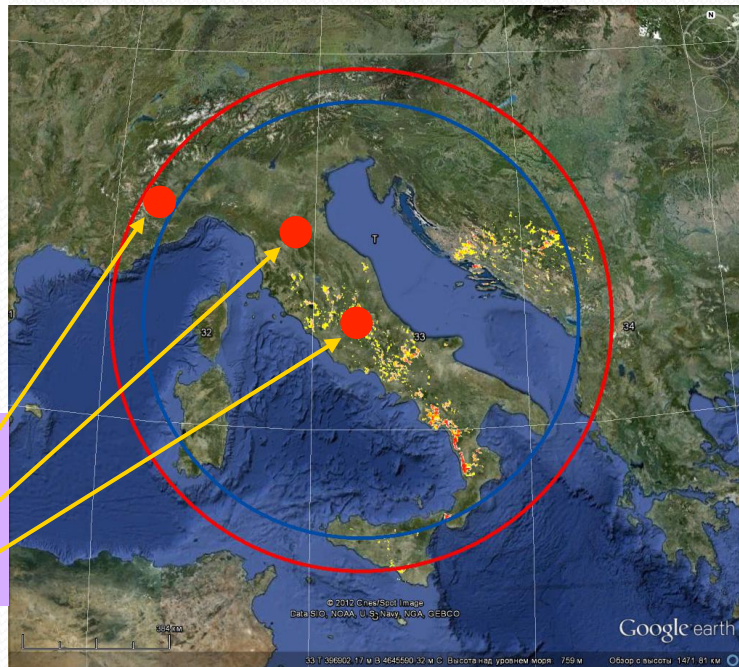
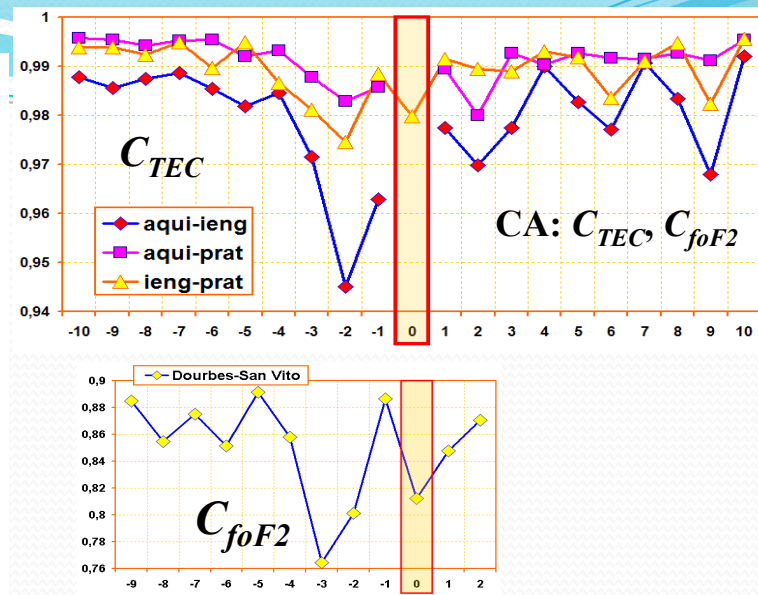
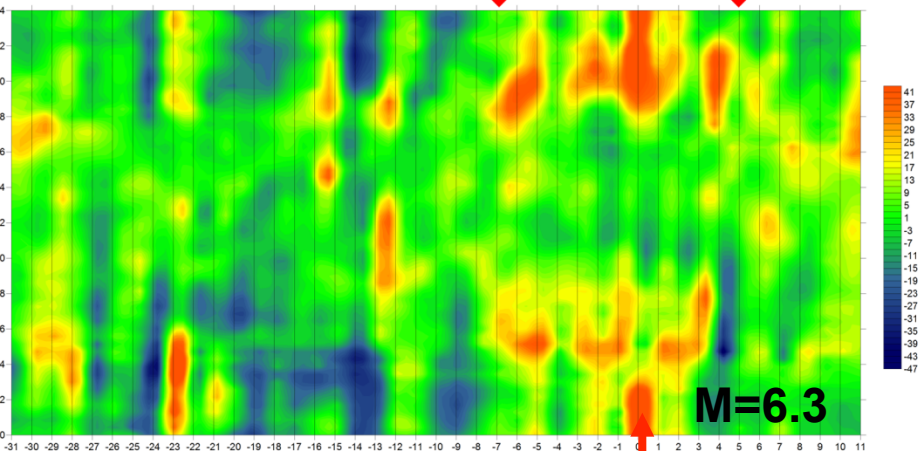
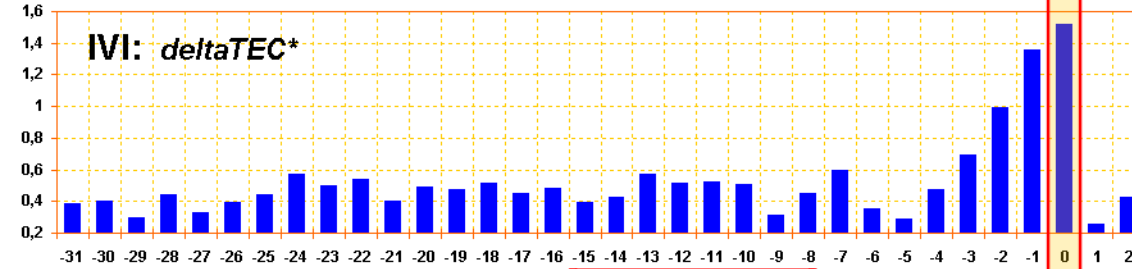
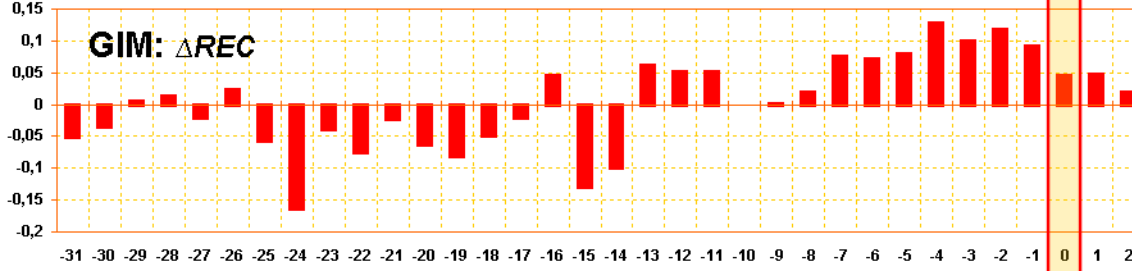
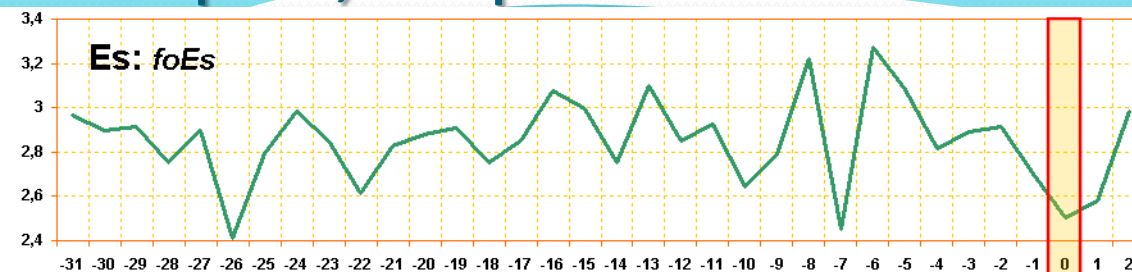
Ionospheric precursor mask for Greece earthquakes with $M \geq 6.0$



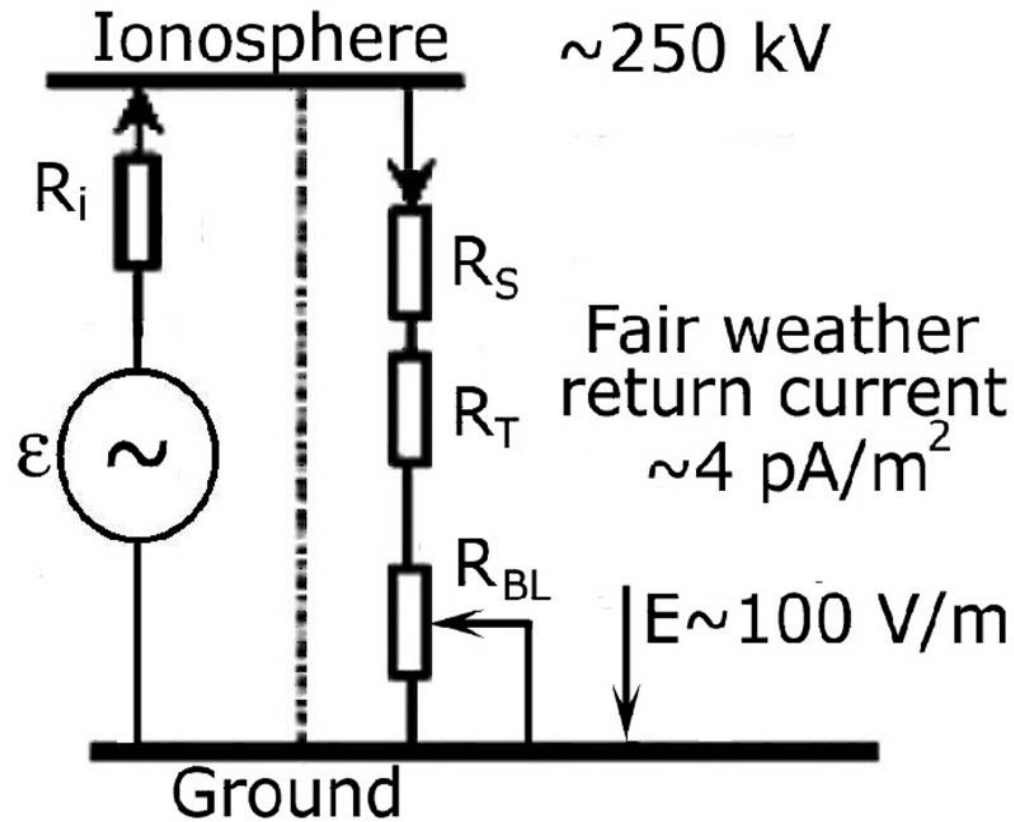
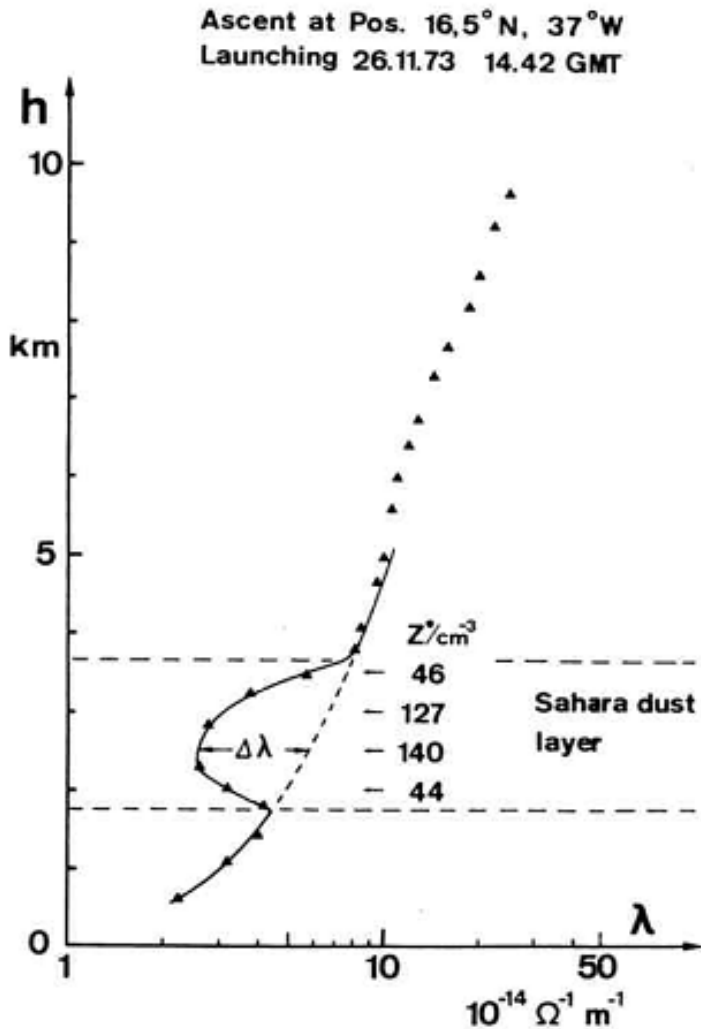
Real time alarms for Greece



L'Aquila, 6 April 2009

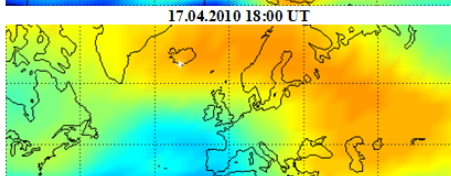
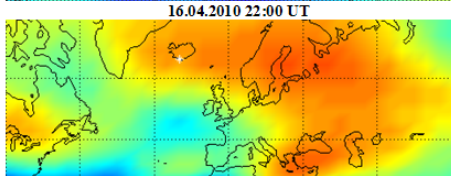
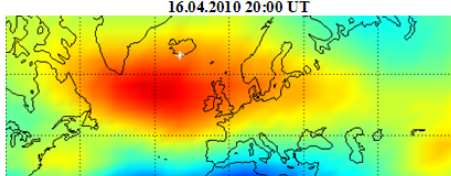
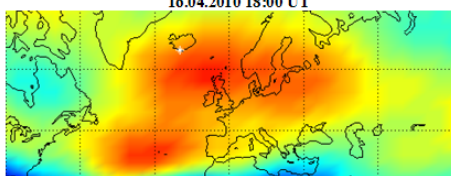
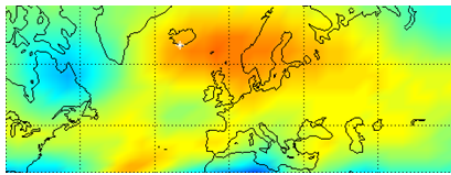


Few words on the physical mechanism

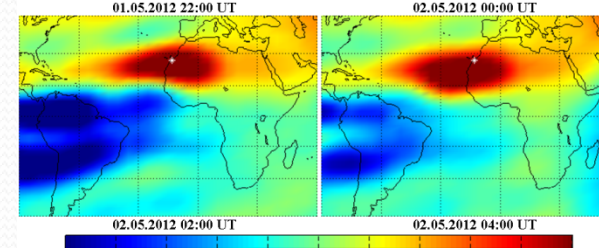
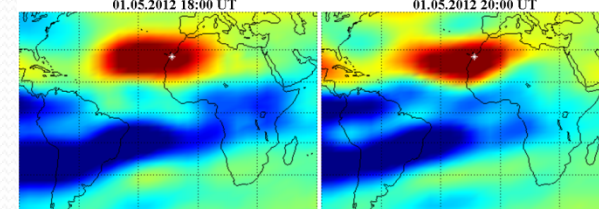
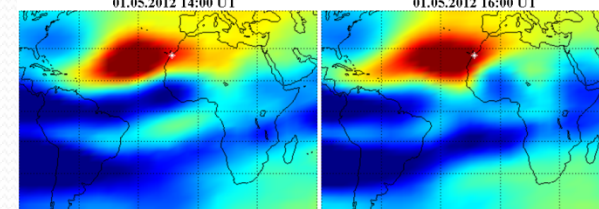
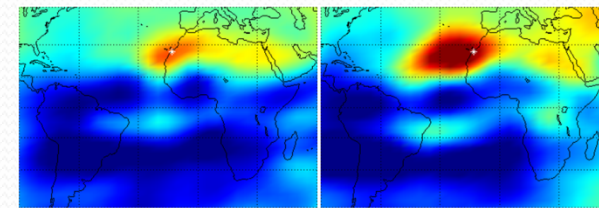
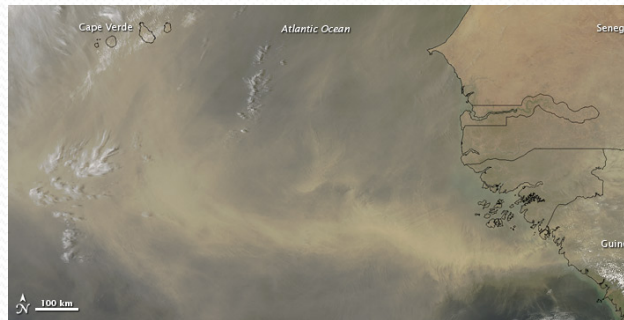


Harrison, 2002

Volcano eruption

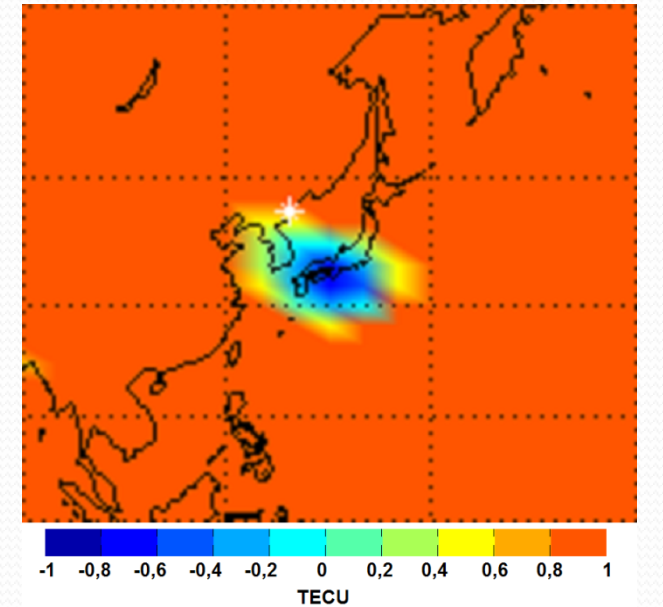


Sand storm



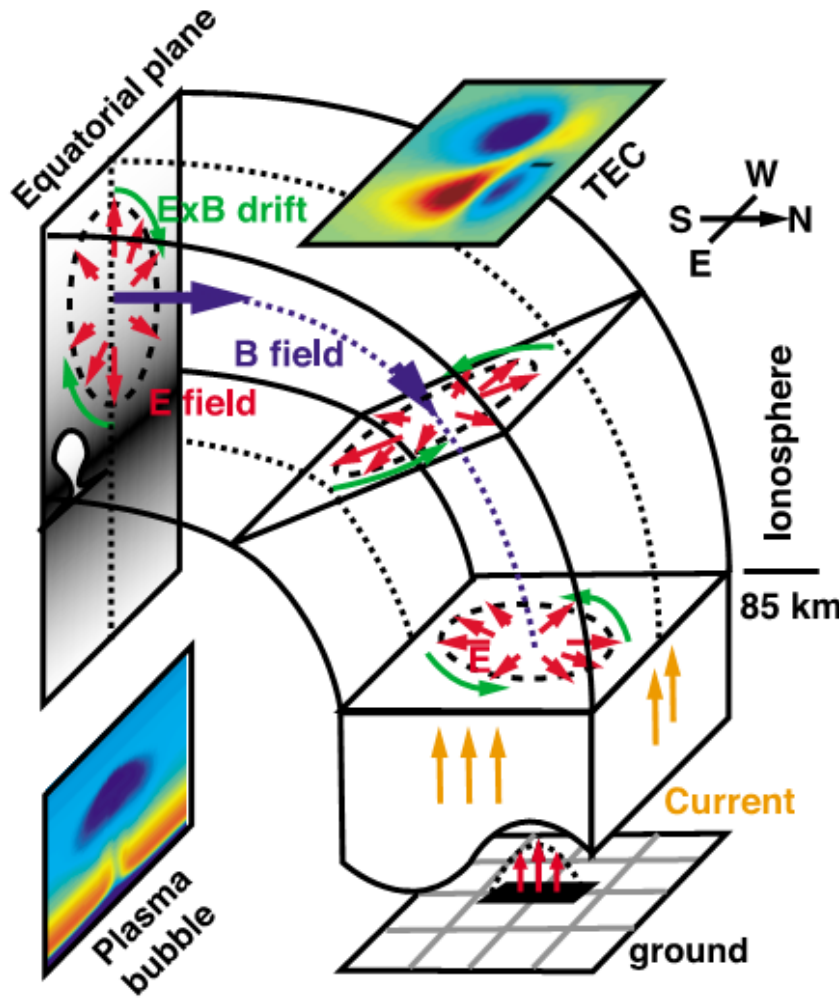
4
3
2
1
0
-1
-2
-3
-4
TECU

Nuclear explosion

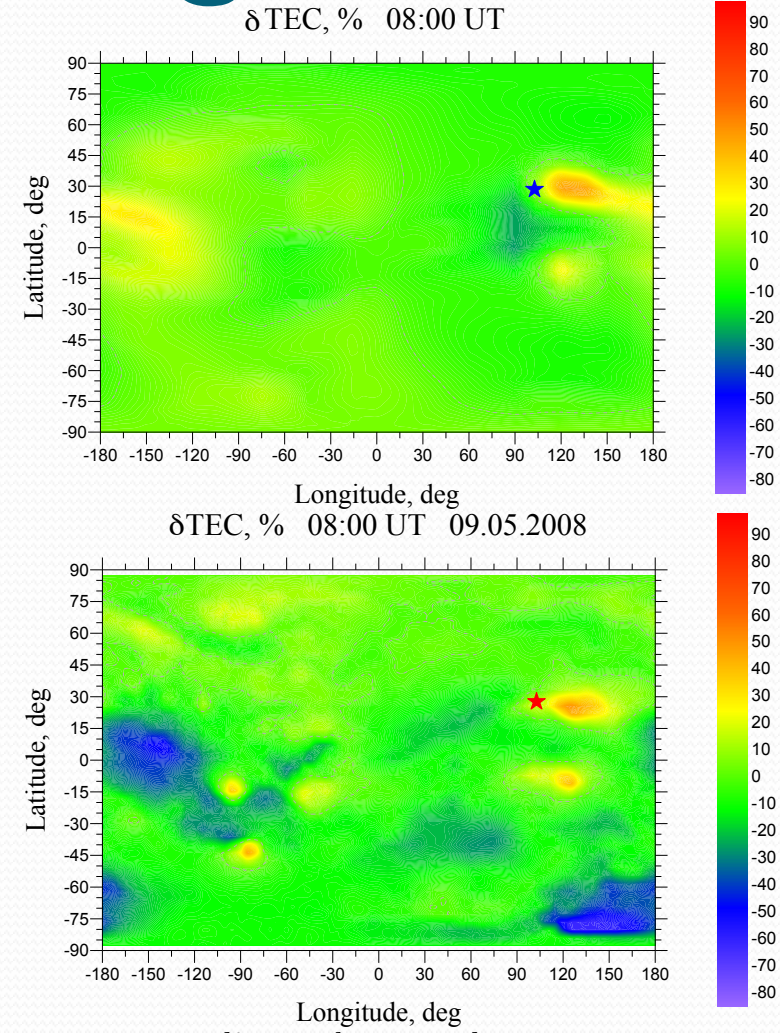


-1 -0,8 -0,6 -0,4 -0,2 0 0,2 0,4 0,6 0,8 1
TECU

Modeling



Kuo et al., JGR, 2011



Klimenko et al., ASR, 2011

3 most comprehensive ionospheric first principal ionospheric models (Huba, Namgaladze, Klimenko) show ionospheric anomalies are of electric field origin

Conclusions

- Seismically induced ionospheric variability is unpredictable from the point of view of ionosphere modeling
- Using the mask conception gives opportunity to automatically identify the regular component of the ionospheric variability associated with seismic activity
- Multiparameter precursors monitoring and precursors synergy permits using the temporal sequence of precursors anticipate ionospheric anomalies using precursors appearing earlier

Thanks for your attention



14 2 2002